UPTEC ES 21038
Examensarbete 30 hp
Oktober 2021

Transmission line protection performance in presence of power electronic-interfaced devices

Impact and needed countermeasures in the Swedish transmission system

Hanna Olofsson

Civilingenjörsprogrammet i energisystem

UPPSALA UNIVERSITET

Transmission line protection performance in presence of power electronic-interfaced devices – Impact and needed countermeasures in the Swedish transmission system

Hanna Olofsson

Abstract

The penetration level of power electronic-interfaced devices (PEID:s) in power systems is increasing, including wind- and solar power, HVDC and FACTS devices. Fault current injected by PEID:s is lower in magnitude, may lack or contain a reduced negative sequence component and can have a wide range of phase angles, as opposed to fault current supplied by synchronous generators (SG:s). In this thesis, the impact of these changes on transmission line protection in the Swedish 400 kV network is investigated trough a literature review and steady-state short circuit simulations.

The literature review shows that residual overcurrent protection and line differential protection works well in presence of PEID:s in most cases. Traveling wave based protection and other fast time-domain protection may be suitable as well. Some type of distance protection on the other hand, are facing challenges associated with their impedance, directional and fault identification algorithms, when PEID:s are the only fault current source. This is partly caused by varying pre-fault grid conditions, lack of negative sequent current and oscillations in fault current magnitude and phase angle caused by the PEID controller. The thesis underlines the need for an increased understanding of specific algorithms included in distance protection in the Swedish 400 kV transmission system, as their performance in presence of PEID:s likely varies between different vendors and year of manufacturing.

Teknisk-naturvetenskapliga fakulteten

Uppsala universitet, Uppsala

Handledare: Anna Pettersson och Niklas Svensson Ämnesgranskare: Mikael Bergkvist

Examinator: Petra Jönsson

Populärvetenskaplig sammanfattning

Vind- och solkraft integreras idag i en allt snabbare takt i elkraftsystemet som en del av den pågående energiomställningen. Dessa kraftslag beror av vindhastighet och solinstrålning, och räknas därmed som variabla energikällor. Till skillnad från kontrollerbara energikällor, så som vatten- och kärnkraft, är en stor del variabel generering ansluten till elkraftsystemet via kraftelektronik, vilket gör att vindkraftgeneratorn och solcellen är elektrisk separerade från elnätet. Kraftelektroniken används för att styra och/eller konvertera elektrisk kraft, där omvandling från likström till växelström eller från växelström till likström är vanliga applikationsområden. Kraftelektronik möjliggör också till exempel transmission med högspänd likström (HVDC).

Vatten- och kärnkraft är anslutna till elkraftsystemet via synkrona generatorer, vilka är stora maskiner som är direkt anslutna till elnätet och som roterar med samma elektriska frekvens som den elektriska nätfrekvensen. När det sker ett fel i kraftsystemet, till exempel en kortslutning där en eller flera faser får elektrisk kontakt med varandra eller med marken, sjunker spänningen i elnätet samtidigt som strömmen genererad av de synkrona generatorerna ökar markant. Denna mekanism är helt baserad på fysikaliska fenomen och strömmen brukar kallas felström. Den förändrade ström- och spänningsnivån vid fel utnyttjas av skyddssystemet i kraftsystemet för att detektera och koppla bort alla fel som uppstår så fort som möjligt. Felbortkoppling görs genom att slå från ledningens strömbrytare. På så vis erhålls drift- och personsäkerhet, samtidigt som så få elkunder som möjligt påverkas av avbrott i elnätet.

Viss typ av vindkraft, solkraft, HVDC och annan elkraftteknik som är anslutna till elkraftsystemet via kraftelektronik benämns power electronic-interfaced devices (PEID:s) på engelska. Dessa matar också ström till följd av fel i kraftsystemet, men felströmmens karaktäristik skiljer sig mycket jämfört med felström matad av synkrona generatorer då den bestäms helt av PEID:ns kontrollstrategi. Till exempel är amplituden betydligt lägre för att skydda kraftelektroniken och felströmmen matas i alla tre faser, oavsett om felet berör alla faser eller inte. Detta har stor påverkan på vissa typer av ledningsskydd som används i det svenska transmissionsnätet, strömmens motorvägar, som förvaltas av Svenska Kraftnät (Svk). Påverkan av felströminmanting från PEID:er på skydd i transmissionsnätet förväntas att bli alltmer signifikant till följd av att mängden PEID:er förväntas att öka i framtiden, samtidigt som mängden synkrona generatorer förväntas minska till följd av kärnkraftsavvecklingen. Detta var bakgrunden till varför Svk initierade detta examensarbete, som syftar till att öka kunskapen om dessa förändringar samt att hitta lösningar på hur potentiell negativ påverkan på skyddssystemet kan undvikas.

Examensarbetet undersöker bland annat hur felströmsinmatning från PEID:er påverkar konventionella ledningsskydd som Svk installerar idag i transmissionsnätet genom en litteraturstudie och steady-state simuleringar. Resultatet indikerar att längsdifferentialskydd och strömmätande jordfelsskyd fungerar väl när PEID:er matar felström, medan vissa distansskydd står inför stora utmaningar relaterat till deras impedans-, riktnings- och fasvalsfunktion. Vidare undersöks också om det finns andra skydd som Svk inte använder idag som kan användas för att öka skyddssystemets pålitlighet. Ett exempel som nämns i litteraturen är så kallade vågbaserade (traveling wave) skydd, som inte är beroende av den stationära felströmmen.

Beroende på nätstruktur och hur man väljer att ansluta PEID:er kommer troligen problematiken för distansskydd att vara olika stor. Skydd av ledningar som ansluter PEID:er radiellt till transmissionsnätet är ett kritiskt fall då PEID:erna är de enda felströmskällorna bakom skydden i den ena änden. Om skyddets funktion för riktningsbestämning och fasvalslogik är tillförlitliga kan distansskydd användas som huvudskydd på båda sidor av ledningen, men möjligheten att stänga av zon 1 på PEID-sidan bör undersökas bland annat i fall där spänningen riskerar att sjunka till en nivå som riskerar skyddets mätnoggrannhet. Snabb felbortkopppling längs hela ledningen kan möjliggöras med hjälp av överräckande skyddssamverkan mellan den starka ledningsänden och änden som ansluter PEID:er. Om det inte går att lita på algoritmerna för riktningsbestämning och fasvalslogik rekommenderas i stället längsdifferentialskydd som huvudskydd för långa och korta transmissionsledningar, i kombination med fjärrutlösning från den starka änden av ledningen för att täcka alla felfall.

Framtida arbeten rekommenderas att undersöka specifika distansskydd i detalj, då de kan fungera olika beroende på skyddsleverantör och tillverkningsår. Det rekommenderas också bl.a. att undersöka skydd för seriekompenserade ledningar med stor andel felströmsinmatning från PEID:er i närheten samt skydd av ö-nät och andra mycket svaga nät.

Executive summary

The penetration level of power electronic-interfaced devices (PEID:s) in power systems is increasing, including wind- and solar power, HVDC and FACTS devices. Fault current injected by PEID:s is lower in magnitude, may lack or contain a reduced negative sequence component and can have a wide range of phase angles, as opposed to fault current supplied by synchronous generators (SG:s). In this thesis, the impact of these changes on overhead line protection in the Swedish 400 kV network is investigated trough a literature review and steady-state short circuit simulations in PSS®CAPE.

According to the result, line differential and residual overcurrent protection works well in presence of PEID:s. The result also indicates that some impedance, directional and fault identification functions included in distance protection risks misoperation, mainly when PEID:s are the only fault current source behind it. For example when PEID:s are integrated to the transmission system radially. If the directionality and fault identification algorithms are reliable, distance protection can be used as main protection on both sides of the line, but the possibility of disabling zone 1 should be explored in some cases. For example when the voltage risks falling below minimum levels for measuring accuracy. Accelerating communication schemes can be used to facilitate fast fault clearing along the whole line in such cases.

If the directionality and fault identification algorithms are not reliable, it is recommended to use line differential protection as main protection for long and short transmission lines, in combination with direct transfer trip from the grid side of the line to cover all faults. Residual overcurrent protection and traveling wave based protection can also be used as it is less dependent on the fault current from PEID:s. Moreover, the simulation result indicates that the occurrence of inaccurate impedance calculations and low voltage levels are less in meshed networks with a high penetration level of PEID:s, provided there is also a significant fault current contribution from SG:s.

For future work, it is recommended to investigate the performance of specific distance protection in detail, as their functions work differently depending on protection vendor and year of manufacturing. Among other things, it is also recommended to investigate the performance of protection on series compensated lines integrating PEID:s radially as well as protection of islanded networks and other very low inertia systems.

Acknowledgement

This thesis project was initiated by Svenska Kraftnät (Svk). I am happy that I was given the chance to investigate this interesting topic for their account, and with that, finish my Masters degree in Energy Systems Engineering. I am very grateful for my incredible supervisors Anna Pettersson and Niklas Svensson at Svk who invested so much time into helping me throughout the duration of this project. Your kindness, patience and expertise has been essential for the completion of this thesis. I also think that we had a good time together during our many skype-meetings. Stort tack!

I would also like to take the opportunity to thank my subject reviewer Mikael Bergkvist for his encouragement and helpful comments on the report. Last but not least, I also wish to thank my friends Madeleine Karlberg and Hilda Andersson-Gran, as well as my sister Sofia Olofsson, for their support and friendship. I appreciate you!

Hanna Olofsson
September 2021

List of Abbreviations

DSO	Distribution System Operator
DTT	Direct Transfer Trip
EMTP	Electromagnetic Transients Program
FACTS	Flexible AC Transmission Systems
FID	Fault Identification Logic
HVDC	High Voltage Direct Current
IED	Intelligent Electronic Device
LL	Line to Line
LLG	Line to Line Ground
PEID	Power Electronic-Interfaced Device
P.U.	Per Unit
PUTT	Permissive Under-Reaching Transfer Trip
POTT	Permissive Over-Reaching Transfer Trip
RES	Renewable Energy Sources
RTDS	Real Time Digital Simulator
SLG	Single Line to Ground
SOFT	Switch onto fault
STATCOM	Static Synchronous Compensators
Svk	Svenska Kraftnät
TPH	Three-phase
TSO	Transmission System Operator
TW	Traveling wave
VSC	Voltage Source Converter
WTG	Wind Turbine Generators

Table of Contents

Chapter 1

Introduction

World-wide deployment of renewable energy sources (RES) continues to increase rapidly due to the ongoing energy transition. According to Wind Europe, 105 GW of new wind energy capacity will be installed in Europe over the next five years [1]. The penetration of RES has already reached high levels in parts of the world, meaning that the installed capacity of RES is high in relation to the total electricity generation capacity in MW. In Sweden, the share of wind and solar power of the installed capacity was 23.5% and 2% respectively in 2020 [2]. In addition, wind power accounted for 17% of the total electricity production the same year [3].

Integration of RES to the existing AC transmission system is enabled by the use of power-electronic converters. These are electric circuits consisting of semiconductor switches used in a wide range of application areas where electric power is to be controlled and/or converted. Amplitude, frequency and phase angle of current and voltage are examples of properties that are commonly altered in power system applications, and the most common conversion is between DC-AC through inverters and AC-DC through rectifiers.

High-voltage direct current (HVDC) links and flexible AC transmission systems (FACTS) are other application areas for power-electronics in the power system. Transmission through HVDC is becoming more utilized because it is well suited for long distance transmission for example, which can be used for integration of offshore wind power and other remote electricity generation plants.FACTS are a group of technologies aimed to enhance voltage and angle stability in the power system. Static synchronous compensators (STATCOM) is a member of the FACTS family, capable of regulating the voltage at the point of connection to a network, through absorption and injection of reactive power.

A large portion of wind- and solar power plants, HVDC links and FACTS can be referred to as power electronic-interfaced devices (PEID:s)[4]. According to fault-ride through requirements established by the transmission system operators (TSO:s), these devices are not allowed to disconnect from the power system within a certain voltage span, when a network fault occurs [5]. In addition, as devices interfaced by voltage-source converters (VSC:s) has the capability of supplying active and reactive power independently, requirements for fast fault current injection are also possible, with the purpose of supporting voltage during faults.

The fault response of PEID:s is partially or fully governed by the grid side converter controller. This is very different compared to traditional fault current injection by synchronous generators (SG:s), arising due to physical phenomenon [4]. The fault response of PEID:s and SG:s have significant differences in terms of fault current amplitude, phase angle, and sequence components among other things. For example, PEID:s inject fault current between 1-1.5 p.u. [4, 6, 7, 8], whereas SG:s inject current between 3-6 p.u. [4]. The fault response of SG:s are predicable, well-understood and provides a clear distinction between normal operation and fault conditions. In contrast, the fault response of PEID:s are inherently non-universal as it is dependent on the controller. Additionally, in the case of power electronic-interfaced generation (PEIG), there are no clear grid codes in Sweden specifying characteristics for fault current injection by these devices. A frequently referenced grid code is the German one, which require positive and negative sequence reactive current injection for unbalanced faults, aiming to support the voltage only in faulted phases [5].

These issues were investigated from a system perspective in a thesis project initiated by Svenska Kraftnät (Svk) in 2020, carried out by Sandra Thengius [4]. The project focused on describing the difference between fault current injection by PEID:s and SG:s, consequences of an increased PEID penetration, as well as what converter control settings can be used to enhance power system conditions during faults. The impact of PEID fault current injection on protection in the power system was discussed and mentioned as an area in need of more research.

The purpose of the protection system is to detect abnormal grid conditions and to isolate faulty components as fast as possible. It is essential to keep people and equipment safe from any type of damage caused by electrical disturbances, and to keep the grid uninterrupted to a high degree during fault events. As a lot of protection equipment installed in the power system today was designed based on theory related to the fault response of SG:s, it is important to investigate how the fault response of PEID:s will impact the protection system. For example, some protection schemes rely on a substantial fault current amplitude, and others depend on certain sequence quantities, which are characteristics of fault current injected by PEID:s that are different from the fault current supplied by SG:s. The impact on protection could possibly be further magnified in the future as the amount of SG:s may decrease in Sweden following shut downs of nuclear power plants, hence, PEID:s will then provide a large portion of the short circuit power. This thesis project will, therefore, explore how reliable fault clearing can be facilitated going forward. Focus is set on protection of overhead lines in the Swedish 400 kV network. This includes how the performance of currently used protection is affected by PEID:s and if there are other protection types, settings or schemes that could improve the performance of the protection system in presence of PEID:s or in highly PEID penetrated networks.

1.1 Objectives

The objective of this thesis is to provide an improved understanding on how power electronic-interfaced devices impacts the existing protection system on transmission level and how identified issues can be mitigated. The aim is to answer the following questions:

i. From a protection perspective, what are the relevant differences between the fault response of PEID:s and SG:s?

ii. What impact does an increased penetration of PEID:s have on transmission line protection in the Swedish 400 kV transmission system?

iii. What changes are needed to ensure a reliable protection system in the Swedish 400 kV transmission network today and in the future?

1.2 Scope and limitations

The scope of this thesis is limited to protection of overhead lines in the Swedish 400 kV transmission system, which is solidly grounded. Typical distribution systems with radial lines and overcurrent protection as their main protection are therefore excluded from this work. In addition, protection functions found in other countries, which are equal to or less advanced than the protection functions currently deployed in the Swedish transmission system, will not be covered. Lastly, the majority of faults in the transmission system occurs on transmission lines, and therefore, protection of other power system equipment such as bus bars and transformers are excluded from the study.

1.3 Outline

The report is structured in 11 chapters that together will fulfill the thesis objective. Chapter 2 and 3 provides a brief introduction to short circuit theory and describes the building blocks of the protection system in the Swedish transmission system today. Chapter 3 provides information on the future outlook of PEID integration, introduces different types of PEID:s and describes fault current injection by PEID:s in relation to SG:s. Furthermore, chapter 4 summarises findings from the literature review related to how the changed system behaviour during faults impacts the current protection system. Chapter 6 continues by introducing other protection schemes with properties suitable in presence of PEID:s. Moreover, chapter 7 describes the model used for steady-state simulations conducted within this thesis. A real wind park and a high PEID future scenario is included. The result from these simulations as well as a brief analysis is presented in chapter 8. Lastly, chapter 9 aims to tie the result together and provide a further discussion on the implications of the results, chapter 10 suggests topics for future work and conclusions are presented in chapter 11.

Chapter 2

Short circuit theory

The following chapter aims to introduce theoretical concepts used for short circuit analysis in this report. First, common fault types and fault resistances is introduced. This is followed by a brief explanation of the concept of symmetrical components, which is used throughout the report.

2.1 Types of faults

Most power system faults are unbalanced/unsymmetrical, meaning that the fault is either only affecting one phase or maximum two, for a three phase system. Furthermore, unbalanced faults can be classified as either shunt or series faults. The later refers to open circuit faults caused by broken conductors or misoperation of circuit breakers for example, but these faults are not included in this thesis.

There are mainly three types of unbalanced shunt faults, where single-line-to-ground (SLG) faults is the most common fault type in transmission systems, followed by line-to-line-ground (LLG) and line-to-line faults (LL). Furthermore, the two main symmetrical fault types are three-phase and three-phase-to-ground (TPH). These faults are more severe than unbalanced faults, but less common. Lastly, according to statistics provided by Svk, most fault occurs on overhead lines caused by lightning strikes. Other causes for unbalanced faults are insulation breakdown and mechanical damage.

2.2 Fault resistance

Shunt faults can be accompanied by fault resistance (R_f), consisting of one or two of the following components: an arc resistance and/or a resistance to ground. In this thesis project, ground resistance of 0, 10 and 20 ohms is investigated because it is covers most earth faults occurring on overhead lines with ground wires, according to Svk:s experience. The arc resistance for LL, LLG and TPH faults can be estimated using Warringtons formula, described in equation 2.1 [9].

$$R_f = \frac{28707 \cdot L}{I^{1,4}} \tag{2.1}$$

where L is the length of the arc in meters, which is equal to the space between conductors initially. This is usually 11m for 400 kV transmission lines in Sweden. When tripping is delayed, for example for zone 2 and 3 faults of distance protection (Introduced in section 3.1), the arc length has time to expand. At Svk and in this project, this length is estimated to be $11 \cdot 3 = 33$ m. Lastly, I is the fault current in amperes.

2.3 Symmetrical components

The method of symmetrical components is used to analyze unbalanced three-phase systems. It is based on a linear transformation of unsymmetrical phase components, to three sets of of symmetrical components: the zero, positive and negative sequence. A set of balanced phasors constitutes only of positive sequence components. The transformation is defined by equation 2.2 for current and 2.3 for voltage.

$$\begin{bmatrix} I_A \\ I_B \\ I_C \end{bmatrix} = \begin{bmatrix} 1 & 1 & 1 \\ 1 & a^2 & a \\ 1 & a & a^2 \end{bmatrix} \begin{bmatrix} I0 \\ I1 \\ I2 \end{bmatrix} \tag{2.2}$$

$$\begin{bmatrix} V_A \\ V_B \\ V_C \end{bmatrix} = \begin{bmatrix} 1 & 1 & 1 \\ 1 & a^2 & a \\ 1 & a & a^2 \end{bmatrix} \begin{bmatrix} V0 \\ V1 \\ V2 \end{bmatrix} \tag{2.3}$$

where index A, B and C refers to the phase current and voltage in the three phase system and index 0, 1 and 2 represents the zero, positive and negative sequence current and voltage respectively. Furthermore, a is a complex number: $a = 1 \angle 120°$. Further description of symmetrical components can be found in reference [10], among many other references.

Chapter 3

Power system protection today

The purpose of a power grid protection system is to detect and disconnect faulty elements in order not to comprise operational reliability and stability, as well as personal safety and to protect power system equipment [11]. Figure 3.1 displays basic components of a fault clearing system. However, additional components enabling proper communication and control are an essential part of the fault clearing system as well.

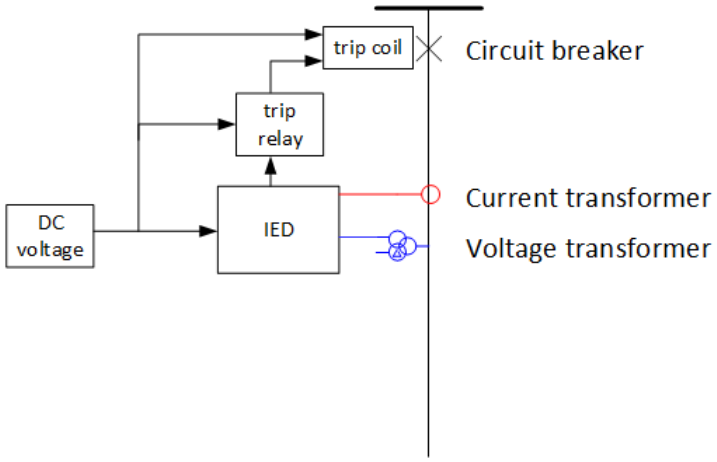

Figure 3.1: An overview of basic components of a fault clearing system.

Current and voltage transformers enables measurements in the transmission grid as they transform high voltage and current to scaled down replicas, that is within operating levels of measuring instruments. The intelligent electric device:s (IED:s) holds microprocessor-based protection functions aimed to interpret these measurements and distinguish between normal and abnormal conditions. Historically, this was done using electromechanical and static protection relays and there are still some of these installed in the Swedish transmission system today, but microprocessor-based protection dominates. Each function in an IED may consist of several sub-functions, for example an impedance and a directional sub-function. The three main protection types in the Swedish transmission grid is presented in latter sections. Furthermore, if a fault is

detected by an IED, a signal is sent to the trip relay, which closes the circuit to the trip coil and the circuit breaker opens.[11]. Svk trips all three phases independently of fault type. Moreover, in this thesis, focus is set on the protection functions constituting the IED:s and the interaction between these devices, as short circuit power characteristics of the power system impacts their functionality.

Speed, *selectivity* and *reliability* are examples of design criterias used by protection engineers. Speed refers to the protection system being able to clear faults fast. The protection system in the Swedish transmission grid is designed to clear faults under 100 ms occurring in normal operation, including both protection IED and circuit breaker operating times. Typically, operating times under 25 ms is required by Svk in the case of distance protection, (Introduced in section 3.1) and the maximum allowed operation time is 40 ms [12].

Fast fault clearing can be conflicting with selectivity, as this term refers to the ability of the protection system to optimize isolation of faults in order to keep the grid uninterrupted to a high degree. One way of insuring reliability is to use primary and back-up protection locally, which is used for all 400 kV transmission lines in Sweden. An additional way is to use remote back-up, secured through overreaching zones of protection, which the in case of transmission line protection means that the protection function is able to detect some faults beyond the line.

3.1 Distance protection

Distance protection uses the ratio of voltage and current, i.e. impedance, to detect short circuits and ground faults on transmission lines. Figure 3.2 shows an example of this protection scheme. Distance protection are placed on both sides of the line, measuring current and voltage. The apparent impedance (Z_{app}) is computed and the result is compared to pre-set impedance characteristics which are based on the line impedance (Z_L) and offline short circuit simulations of the power system in question.

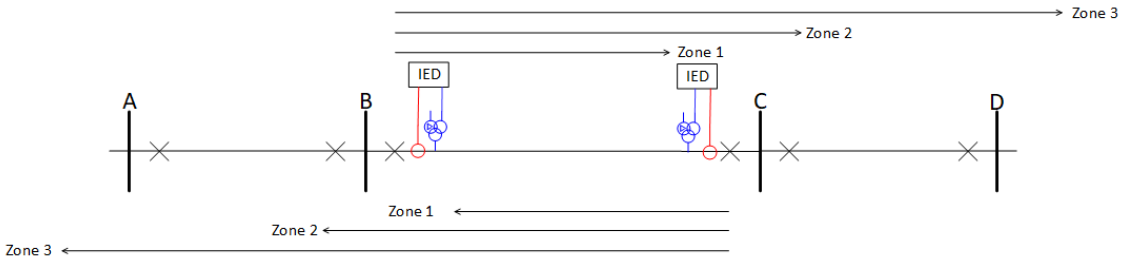

Figure 3.2: A typical distance protection scheme, including three forward zones.

Basic distance protection schemes usually consists of one instantaneous directional zone and at least one time-delayed zone [11]. The example scheme displayed in figure 3.2 consists of three protective zones, all of which are directional, which means that they detect faults only in one direction. In addition, a non-directional and instant switch onto fault function (SOFT) is used by Svk with the purpose of providing fast tripping in cases where the circuit breaker is closed on a fault. In the Swedish transmission grid, zone 1 usually covers 85% of the line and operates instantly if $Z_{app} < Z_R \cdot 0{,}85$. Zone 2 usually covers at least 120% of the line impedance in order to work as remote back-up for the remote bus. This zone is time-delayed by

0.4 s and operates if $Z_{app} < Z_L \cdot 1{,}2$. Lastly, zone 3 is normally set to provide remote back-up for transmission lines emanating from the remote station with a 1.2 s time delay.

Typically, equation 3.1 is used to calculate the impedance for short circuits and equation 3.2 and 3.3 is used in the case of ground faults. However, there are other ways to calculate the apparent impedance too and different vendors may use different ones.

$$Z_{app} = \frac{V_A - V_B}{I_A - I_B} \tag{3.1}$$

$$Z_{app} = \frac{V_A}{I_A + K_n \cdot 3I0} \tag{3.2}$$

$$K_n = \frac{Z_{L0} - Z_{L1}}{3 \cdot Z_{L1}} \tag{3.3}$$

where V_A and V_B is the phase to ground voltage in the faulted phases, I_A and I_B is the phase current in the faulted phases, I_0 is the zero sequence current and K_n is the the zero sequence compensation factor. This factor is used to secure ground fault detection. In equation 3.3, Z_{L0} and Z_{L1} refers to the zero and positive sequence impedance of the transmission line.

Svk uses distance protection based on quadrilateral characteristics, where it is possible to choose restive and reactive reach independently of each protective zone. In addition to computing the apparent impedance, distance protection may use negative or zero sequence quantities to determine fault direction as well as faulted phase, i.e. type of fault. Other supervision elements may occur as well, for example the power swing function used to distinguish between faults and power swings and over-current supervision that prevents distance protection to operate if the current level is too low. The former function is not used often by Svk. Lastly, all sub-functions is a part of the same IED.

3.1.1 Communication schemes

Communication-assisted protection refers to protection schemes utilizing communication between IED:s at each end of the protected unit, with the purpose of decreasing the fault clearing time. The following section will introduce the communication schemes used by Svk today, but it should be noted that there are other types as well. In this section, the protection device at each end of the transmission line is refered to as unit A and unit B.

One of the simplest communication scheme is the *Direct Transfer Trip* scheme (DTT) and this scheme is sometimes used on radial lines in the Swedish transmission system. If a fault is detected by unit A, a trip order is sent to unit B, which trips immediately after received signal. If the fault was located close to unit A (zone 2 for unit B), unit B would trip the fault after an initial time-delay of 0.4 ms if not DTT was used. Even if this scheme has a great potential of decreasing fault clearing time, it may also lead to unwanted trips due to accidental operating or malfunctioning communication equipment, and therefore, DTT is not widely used [11].

Permissive Under-Reaching Transfer Trip (PUTT) schemes is a communication scheme used by Svk, which work through two-way communication. If unit A detects a zone 1 fault on the line, it tells the remote IED to trip fast if it also detects a fault. This means that the remote protection IED can trip without time-delay, for a zone 2 fault. PUTT can be viewed as a DTT with supervision by the remote IED. *Permissive Over-Reaching Transfer Trip* (POTT) is another two-way communication scheme that works in a similar way. However, this scheme does not need a zone 1 pick up to initiate acceleration pulses. For example, if unit A pick up in zone 2, it will send a trip signal to unit B. If it also detects a zone 2 fault, it is allowed to trip fast [11].

Weak infeed logic can be used as a compliment to POTT for transmission lines where one end interfaces a weak source and the other interfaces a strong source. At the weak end, the communication scheme is supplemented by not only sending an acceleration pulse when starting a forward-facing zone but also when an acceleration pulse is received from the strong end [11]. However, an acceleration pulse is not sent if the weak end has detected a fault in a backward zone. The weak infeed logic can also include remote tripping from the strong end, which is enabled if the acceleration pulse is echoed by the weak end. This is often also supervised by a under-voltage criteria at the weak end.

3.2 Differential protection

Differential protection are commonly applied to transformers, generators, busbars, short transmission lines (typically $\lessapprox 25$ km in the Swedish transmission grid) and cables. They are based on Kirchhoff's current law, i.e. that the sum of current entering and leaving the same junction equals zero. Therefore, current is measured at each end of the line and compared numerically through a differential protection function. Unlike distance protection, differential protection is a so called unit protection scheme, which means that they only detect faults on the protected object and cannot be used for remote back-up of other objects. A distinction between line differential and distance protection is that differential protection need well working communication channels and time synchronized measurements, whereas distance protection can work independently of protections at the other end of the line. However, as described in section 3.1.1, communication between distance protection can enhance their performance.

The maximum allowed differential current differs depending on the current level. Figure 3.3 displays an example of a line differential chart and it is apparent that the allowed differential current is larger for larger fault current levels (restrain current). However, these characteristics can be different for different grid topologies and protection manufactures. In this project, the differential and restrain current is defined by equation 3.4 and 3.5.

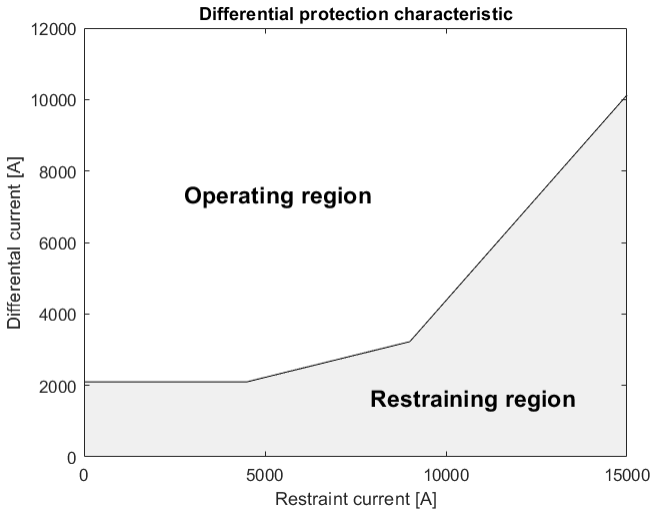

Figure 3.3: A typical differential protection characteristic chart used by Svk.

$$I_{diff} = abs(I_A + I_B) \tag{3.4}$$

$$I_{res} = max(I_A, I_B) \tag{3.5}$$

3.3 Residual overcurrent protection

The residual overcurrent protection is used to detect ground-faults through measuring the residual current, which by definition is the sum of the three-phase currents. It normally consists of four steps; three directional and one non-directional. These steps can be seen in figure 3.4. It operates if the measured residual current exceeds a threshold during a pre-set duration time. Step 1, 2 and 23 has definite time functions of 0, 0.4 and 0.8 s respectively. The current thresholds for each of these steps are based on zero sequence current obtained through simulations of ground faults and are therefore dependent on the grid topology. Step 3 uses an inverse time delay curve to ensure selective disconnection even for high ohmic ground faults. The current threshold of this step is standardised to 120 A independent of the grid topology in the 400 kV transmission system. Moreover, communication schemes presented in section 3.1.1 are often used to enhance the performance of these protection devices.

Svk has recently decided not use stage 1 and stage 2 in new installations. The reason for this is the increasing difficulty to find proper settings in a power system with higher fluctuations in fault current level and that they are not needed any more as modern distance protections can fully replace their function.

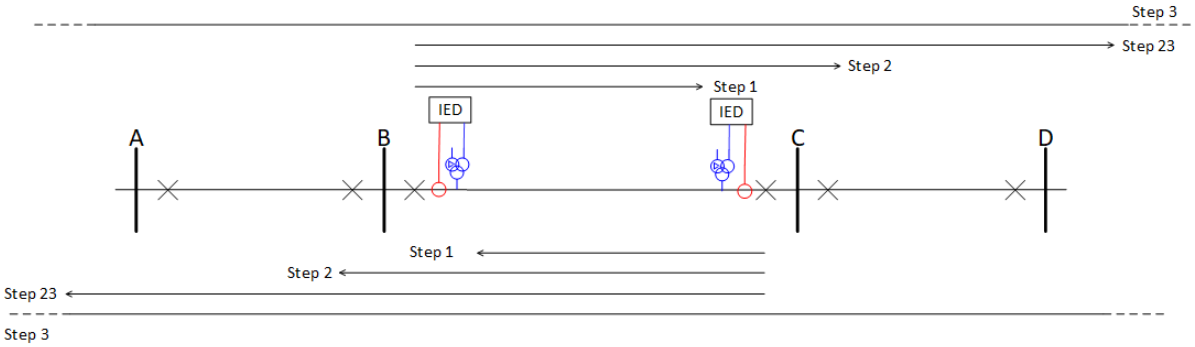

Figure 3.4: A typical residual overcurrent protection scheme used by Svk.

Chapter 4

PEID background and fault response

The following chapter will first present trends and possible future scenarios of renewable energy production in Sweden. Next, a brief introduction is given to some common types of power electronic-interfaced devices. Thereafter, the fault response of PEID:s is described, which is important in order to understand how the protection system is impacted by PEID integration. In this way answering objective i, i.e. present differences between the fault response of PEID:s and SG:s that are relevant from a protection perspective.

4.1 Trends and forecasts

Renewable energy production is increasing significantly world wide thanks to its low climate impact, technology advancements and cost reduction. Figure 4.1 displays data on global wind- and solar power capacity between the year of 2009-2019, obtained from the International Renewable Energy Agency [13].

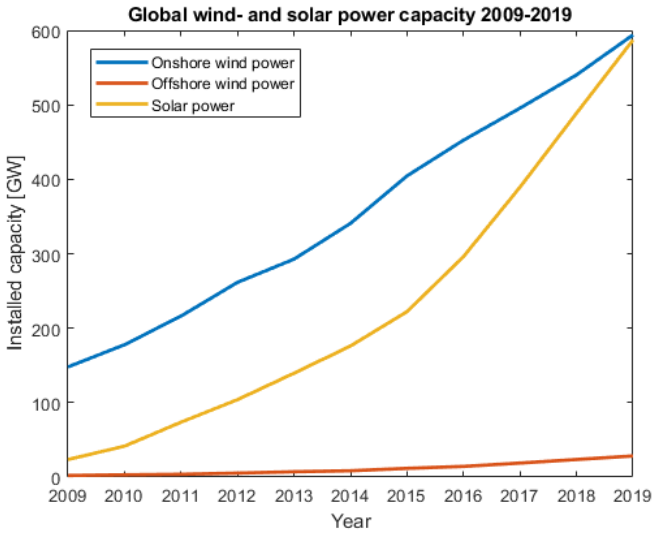

Figure 4.1: Cumulative wind- and solar power capacity world wide 2009-2019 [13]

In May of 2021, Svk published a long-term market analysis, focusing on possible future scenarios for the Nordic and northern European power system until the year of 2050. Four scenarios are analyzed from various aspects with the intention of identifying future needs and challenges for the power system. Figure 4.2 displays assumed capacities for each energy type in 2045, according to each scenario included in the long-term market analysis. Capacities in 2020 is included in the figure as well in order to be used as reference.Orange/red is used for energy types likely connected to the power system via synchronous generators and blue represents energy types likely interfaced by power-electronics.

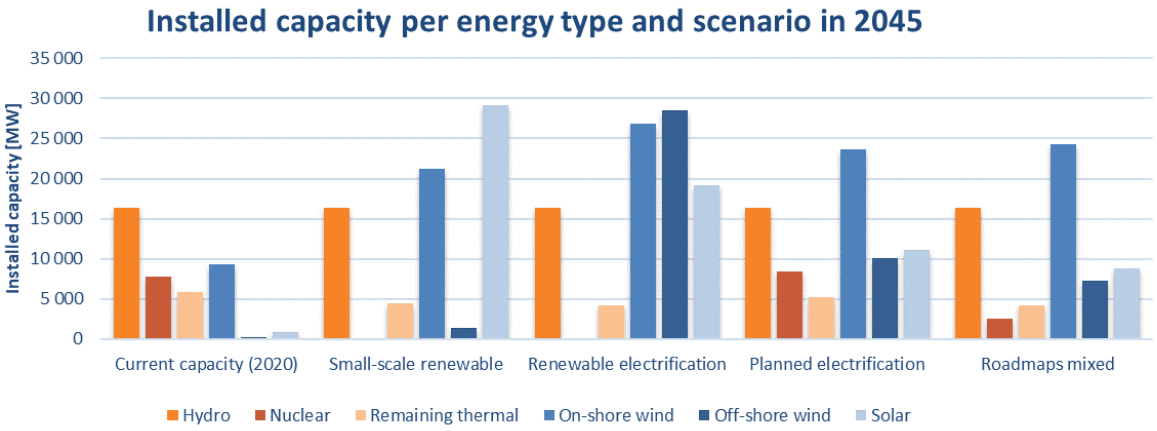

Figure 4.2: Installed capacities in Sweden in four different scenarios, for the year of 2045 [2].

It is likely that scenario *Renewable electrification* or *Small-scale renewable* will introduce the most challenges to the protection system in 2045 due to nuclear power decommission and the extensive RES capacity increase. One key difference is that more RES is likely to be integrated on higher voltage levels in scenario *Renewable electrification*, as this is common for large-scale wind power. This is likely to make the fault response of PEID:s very noticeable on transmission level. In scenario *Small-scale renewable* on the other hand, much solar power can be interpreted to be integrated on low voltage levels, which could mean that the impact of PEID:s is less noticeable on transmission level, but the strength of the transmission system could be lower than in scenario *Renewable electrification*.

Another important view-point is the geographical distribution of fault current sources. For instance, in the market analysis, the capacity of hydro power is assumed to be constant between the years of 2020-2050. As a large portion of hydro power is located in northern Sweden, the protection system in the south of Sweden may be more affected by PEID:s in 2045 than in the two previously discussed scenarios. This is the motivation for using capacities in SE4 (A bidding area in the south of Sweden) for the scenario *Renewable electrification*, as inspiration to a short circuit model produced in this thesis project, which is presented in section 7.5. Specific data for each bidding area is not published in the long-term market analysis [2], but these values were obtained from Svk.

4.2 Types of PEID:s

The following section will introduce different types of PEID:s used in power system applications. Other common terms used to describe some types of PEID:s are inverter-interfaced renewable energy generators (IIREG), inverter-based resources (IBR), inverter-interfaced generators (IIG) and converter-interfaced generation (CIG).

There are mainly two types of wind turbine generators (WTG) on the market today: doubly-fed induction generators (DFIG or type III) and full-size converter WTG:s (type IV), both utilizing power electronics to connect to the grid [14]. According to data provided by Svk, 25% and 75% of wind power connected to the Swedish power grid is of type III and type IV respectively. This data does not include all WTG:s, but gives a good indication on how the distribution between WTG types looks like today. More precisely, it includes mainly larger parks (>30 MW) connected to voltage levels of 70 kV or higher.

Three different types of power electronic-interfaced generation can be seen in figure 4.3. First, it can be seen in sub-figure 4.3a that the stator of the type III WTG is directly connected to the grid, whereas the rotor is connected through AC-DC-AC conversion. In contrast, a type IV WTG:s and solar PV are fully connected via AC-DC-AC converters, which can be seen in figure 4.3b and 4.3c. This means that their generator/solar panel are electrically decoupled from the rest of the grid, making their fault response different compared to type III WTG.

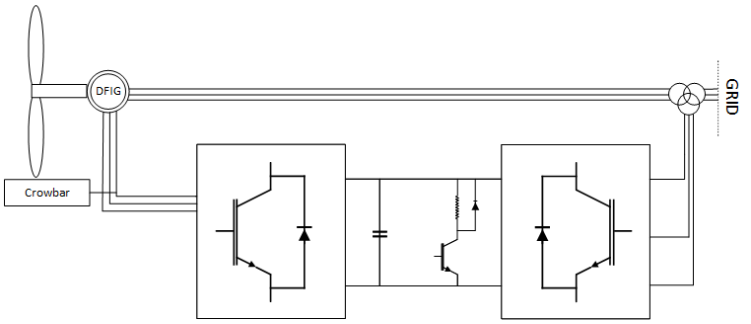

(a) Type III WTG.

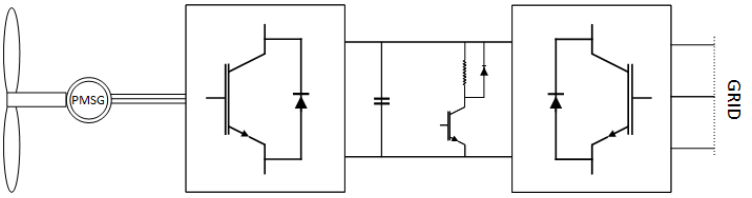

(b) Type IV WTG.

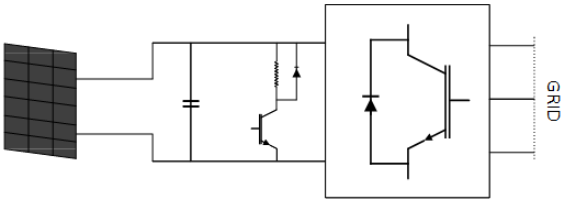

(c) Solar PV.

Figure 4.3: Basic configurations of power electronic-interfaced generation.

As previously mentioned, HVDC is a common way to connect remote electricity production, because it can transfer electricity over long distance with low losses. There are mainly two types of converters used in modern HVDC transmission systems: current source converters (CSC:s) and voltage source converters (VSC:s). The former uses thyristor valves and the latter utilizes insulated-gate bipolar transistors. One key difference between these technologies is that VSC:s are able to control active and reactive power, whereas CSC:s is capable of controlling only active power. Another important application area for VSC-HVDC is connection of remote offshore wind farms as VSC-HVDC enables island operation. In this report, VSC-HVDC is treated exclusively because their control abilities enables fault reactive current injection as a response to abnormal grid conditions [15]. The basic configuration of a VSC-HVDC link can be seen in figure 4.4.

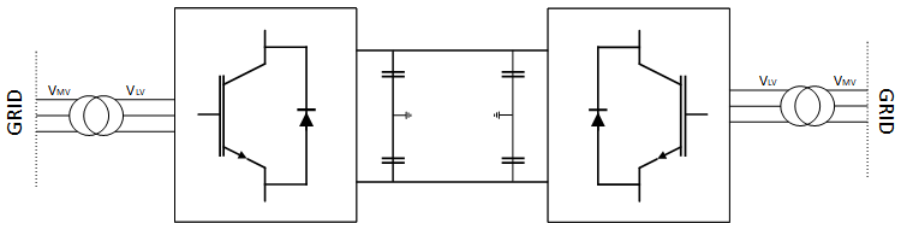

Figure 4.4: Basic configuration of VSC based HVDC.

Another application area for power-electronics in the power system are FACTS, aimed to enhance voltage, angle, and frequency stability in the power system. STACOM is one member of the FACTS family, capable of regulating the voltage at the point of connection to a network, through absorption or injection of reactive power. This device is also connected to the grid through VSC:s [16].

4.3 Fault response of PEID:s

The fault response of PEID:s are to a large extent defined by controller settings, which to a minimum are based on thermal ratings of components. In addition, pre-fault operating conditions and voltage levels has an impact on the response. As previously mentioned, the response is significantly different compared to the fault response of SG:s, which arise solely due to physical phenomenon and has provided the majority of short circuit power traditionally [4]. Moreover, SG:s can be modeled as constant voltage sources behind a reactance, but this model does not hold for PEID:s. Instead they can be viewed as non-linear voltage dependent current sources [17].

As type IV WTG:s, solar power plants, VSC-HVDC and STATCOM are interfaced by full-scale voltage-sourced converters, their fault response is assumed to be similar. Type III WTG:s has to be treated separately due to its configuration and because the response is dependent on the operation of the crowbar, which is a device used to disconnect the rotor from the converter during severe faults in order to protect the power electronics constituting the converter. The response of these machines are similar to the contribution of induction machines during severe faults. When the crowbar does not operate, during faults of low severity, the fault current contribution is similar to the contribution from a type IV WTG. However, the crowbar can be activated and deactivated within a cycle, continuously during a fault, making their response difficult to describe in general terms [14].

The following sub-sections aims to first introduce steady-state fault response characteristics that distinguish PEID:s from SG:s, which are important from a protection point of view. Thereafter, the fault response evolvement of full-converter interfaced devices is introduced, as the response and computation time of the converter prevents control set points to be reached instantly following a fault. Lastly, a difference related to voltage is explained.

4.3.1 Steady-state fault current characteristics

Magnitude

In short, SG:s typically injects fault current between 3-6 p.u. on generator base, in some cases up to 10 p.u., for low impedance faults [4]. This means that traditionally, there has been a significant difference between load current levels and short circuit currents, which simplifies operation of current based protection schemes. PEID:s on the other hand, are limited to inject current between 1.1-1.5 p.u. on unit base [4, 6, 7, 8]. As previously described, type III WTG will behave differently depending on whether the crowbar is activated or not. Reference [14] shows an example where the crowbar is activated during the first 40 ms of a three-phase fault, and is thereafter deactivated during the reminder of the fault time. In that case, the magnitude reached 3 p.u. initially and stabilized at 1.2 p.u. when the crowbar was removed.

Phase angle

Due to the inherent inductive nature of SG:s, the fault current injected by these machines are predominantly inductive. Generally, the fault current phase angle relative to the voltage can be assumed to be between 80-90 °for most fault scenarios, according to experiences of Svk. On the contrary, PEID:s are able to inject current at a variety of phase angles, depending on pre-fault grid conditions, type of fault and control strategy. One common control mode is dynamic reactive current injection, which is based on the change in voltage at the terminal of the PEID, caused by the fault. If the voltage drops, the PEID will inject reactive power to support the voltage. On the other hand, if the voltage increases following a fault, the converter will consume reactive power for the same purpose. Depending on the pre-fault power production and controller, the current can be partly resistive as well [18].

Sequence quantities

Short circuit analysis of networks with synchronous generation assumes that in addition to positive sequence fault current generated by the generator, negative sequence fault current (for unbalanced faults with or without ground) will also flow. Due to the transformers, zero sequence current is also present for grounded faults, which is also the case for PEID:s typically. This means that fault current will only flow in the faulted phases and in connections to ground for grounded faults. This is not the case for PEID:s, as the negative sequence current contribution depends on the PEID type and control settings, but in general they will either partially or fully suppress it. Only a few national grid codes, the German grid code for example, demands inductive negative sequence current injection for unbalanced faults [19]. However, the converter current limit is applied to the phasor sum of positive sequence current (active and reactive) and negative sequence current in any given phase, hence, the negative sequence current is limited even if it is demanded.

4.3.2 Response evolvement

The fault response of full-converter interfaced devices consists of three stages: the initial transient, the transition period and steady-state, accordning to reference [20]. The initial transient occurs between fault inception and when the converter controller recognizes the fault condition and switches control mode. During this period, the firing angle of the power-electronics remains the same as the pre-fault state. Since the terminal voltage has dropped in one or several phases following fault inception, the magnitude of injected current will increase in needed phases. During this period, current limits can be exceeded and it can consist of both positive and negative sequence components. According to results found by reference [21] for an LL fault, the peak current values reached 3 p.u. during the initial transient. Furthermore, the injected current during this stage is similar regardless of control strategy, and it is only depend on the fault scenario and the response time of the converter [20]. According to reference [20], this period lasts between 7-20 ms.

After the initial transient, a transition period occurs, which lasts between 20-30 ms according to reference [20]. The converter acts to control the firing angle of injected current according to the control strategy during this stage, and the current magnitude slowly decays before reaching steady-state. I.e, the transition period refers to the time between when controls are initiated and steady-state is not yet reached. Because integral equations constitutes the controller, oscillations in magnitude and phase angle of the injected current

can occur during this period. In addition, even if the control strategy include negative sequence current suppression, the fault current in this stage still includes a mix between negative and positive sequence components. Detailed analysis of the dynamic response of the PI regulator used has to be performed to obtain detailed phasor information during this stage [20].

After the transient period, steady-state is reached, where the fault response is characterized by current and voltage presented the in the previous sub-section. According to reference [20], this stage should be reached after 27-50 ms. According to reference [5], reference [4], and a protection vendor consulted in this project, steady state should be reached within 20-40 ms after fault inception. The steady-state response lasts until fault clearance or until fault-ride through requirements no longer applies. Furthermore, figure 4.5 displays the minimum and maximum duration of each stage, in relation to operating times of distance protection without delay, e.g. zone 1 distance protection. This zone risks making decisions based on phasors during the initial transient or the transition period. Zone 2 distance protection, that includes a 0.4 s time delay, is therefore not affected by current and voltage during the initial transient or transition period.

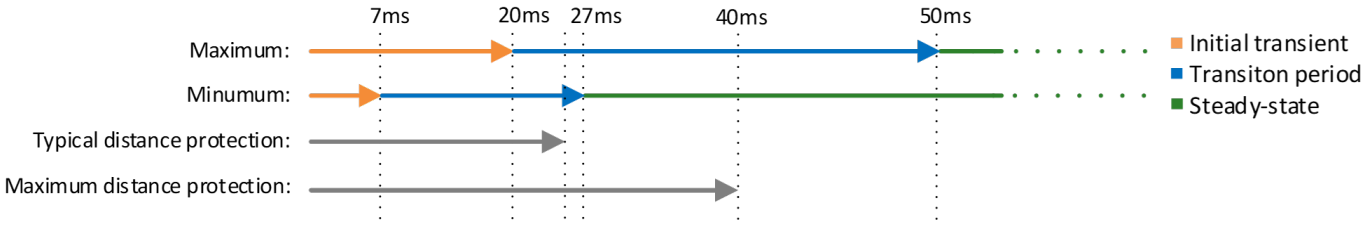

Figure 4.5: Minimum and maximum duration of converter fault response stages according to [20], in relation to typical distance protection operating time and the maximum operating time required by Svk.

4.3.3 Voltage phase angle jumps

Another difference between SG:s and PEID:s is related to the angle of voltage pre- and post fault inception. The source emf of SG:s prevents the voltage angle to change substantially even during short circuits. PEID:s on the other hand lacks consistency and has no physical limit in this regard because the response is dependent on the controller. As a consequence, the fault response of PEID:s may produce phase angle jumps, meaning that there is a substantial difference between the voltage phase angle before and after fault inception [22]. This may be caused by lack of inherent rotational inertia in the power system and resulting fast converter control responses [23]. Most converters are programmed not to produce phase angle jumps, but it is possible and should be noted therefore [22].

Chapter 5

Impact on conventional protection schemes

The following chapter summarizes findings from the literature review conducted within the project with the purpose of answering objective ii and iii, i.e. the impact of PIED:s on transmission line protection and possible mitigation strategies of negative impact. As a compliment, a questionnaire was sent to three vendors of protection equipment used by Svk, but none of them was able to provide answers in writing. Partially due to confidentiality. However, some questions were answered briefly verbally and these answers will also be presented in the following chapter. The questionnaire without answers can be found in appendix A.

5.1 Line differential protection

As previously mentioned, line differential protection operates depending on the sum of current entering and leaving the protected line. Despite uncertainties and differences associated with fault current supplied by PEID:s compared to SG:s, several references claim that it will not threat the functionality of line differential protection [19, 5, 22, 15]. Two vendors has also expressed that line differential protection will be able to operate reliably despite an increasing penetration of PEID:s. If communication channels between measuring points and the IED remain intact, line differential protection will operate for internal phase and ground faults, and restrain for external faults. However, this is not true for very high fault resistance cases, but this is a known problem unrelated to PEID fault current characteristics [19]. Reference [5] recommends a time-delayed phase-phase under-voltage protection and direct transfer trip from distance protection at the remote terminal as back-up protection if communication equipment fails.

Reference [24] studies the impact of PV power plants on line differential protection and found other risks. It concludes that the protection scheme will operate correctly if the phase current on one side is nine times larger than on the other side. i.e. line differential protection benefits from having one weak end, but risks inaccurate operation with two weak ends. The latter is a case where the restrain and the differential current both are low, risking entering the restrain region, seen in the chart displayed in figure 3.3. The same article investigates the influence of the phase angle of fault current injected by PV converters. The result shows that the difference in phase angle between current on both sides can become larger than 90° in cases of short circuits if PV:s are the main fault current source to one side, which could lead to misoperation [24].

The fundamental function of differential protection works the same regardless of manufacturer, even if slightly different algorithms are used. Additional functions can be included however, to further increase reliability of the protection unit, and these functions varies between manufacturers. For example, one vendor consulted within this thesis project mentioned the use of a negative sequence current criteria in some of their differential protection. If the negative sequence current is below a threshold, the differential current is not computed. This could be the case if PEID:s that suppresses negative sequence current are the main fault current source. A solution for this problem could be to switch off this function, or to decrease the setting.

5.2 Distance protection

There are several ways an increasing penetration of PEID:s may reduce reliability of distance protection: due to misoperation related to impedance calculations, direction determination, faulty phase selection, among other things. It was found in [21] that distance protection is the most affected protection scheme used on transmission level in high penetration scenarios of type IV wind power and VSC-HVDC.

5.2.1 Impedance function

Unlike SG dominated networks where the source impedance can be viewed as a predictable system property, the source impedance of PEID:s will change dynamically. This will complicate zone boundary settings for distance protection in some PEID scenarios, especially in cases with radially connected PEID:s [15] and very highly PEID penetrated systems. Reference [21] shows that because the impedance measurement is variable during the transition period, when the converter has detected a fault but the steady-state response is not yet reached, distance protection trips can be unpredictable. Trips could just as easily be initiated but delayed, or refused in a fault scenario. This was investigated using a real time digital simulator (RTDS) and Hardware in the Loop (HIL) tests, using distance protection from different vendors and comparing the performance in a SG dominated and 100% PEID network. According to the same article, false trips in zone 1 for zone 2 faults cannot be ruled out either, but this was not proven in the article.

Reference [25] discusses the increased influence of fault resistance on the apparent impedance measured by distance protection, caused by PEID fault current characteristics. This can be described using equation 5.1 on the system described in figure 5.1. Z_{app} is the apparent impedance measured by distance protection located at bus A, V_A and I_A are voltage and current measured by this protection unit, Z_{AF} is the line impedance between bus A and the fault location, and lastly, I_F is the fault current and R_F is the fault resistance. The limited current injected by the PEID makes the ratio I_F/I_A high compared to if I_A was supplied by conventional short circuit sources of comparable capacity, which results in a big difference between the correct electrical distance Z_{AF} and the apparent impedance Z_{app}. If there in addition is a large phase angle difference between I_F and I_A, a significant reactive part is introduced to the the apparent impedance. As previously discussed, the current I_A is regulated by the control logic of the converter, depending on the type of fault and pre-fault operating conditions. This makes it possible for different Z_{app} to be measured for faults at the same location with equal fault resistance, which therefore complicates zone boundary settings of distance protection.

$$Z_{app} = \frac{V_A}{I_A} = Z_{AF} + \frac{I_F}{I_A} \cdot R_F \tag{5.1}$$

Figure 5.1: A transmission line integrating a PEID radially to a strong system.

A protection vendor mentioned that distance protection in meshed or looped networks including PEID:s should be treated similarly to distance protection in traditional power systems, provided that SG:s is also present in the system in adequate levels. Radially connected PEID:s on the other hand has to be treated differently. The vendor mentioned that misoperation may occur for faults including a fault resistance of 10 ohms or higher. The vendor continued by stating that there is no solution that fits all cases, but speculated if switching off zone 1 could be an option if line differential protection was installed on the transmission line in question. This is especially relevant for shorter lines, as the risk of overreach increases with decreasing line length.

Intermediate infeed by PEID:s is discussed in reference [26]. For a fault along line BC, the apparent impedance detected by the distance protection located at bus A (Z_{app}) can be described by equation 5.2 and figure 5.2. In reference [26] it is shown that possible angular differences between I_A and I_{PEID} can lead to unconventional impact on the apparent impedance. When the local current and the intermediate infeed is supplied by synchronous generators, their phase angle in respect to voltage can be assumed to be between 80-90 °, making the angle of the current ratio to be close to zero. Therefore, the angle of the additional impedance in equation 5.2 is determined by the angle of the line impedance up to the fault Z_{BF}. On the contrary, if there is a large difference between the local current and intermediate infeed, the current ratio has an impact as well. Reference [26] even shows that PEID:s can cause the apparent resistance to be negative due to this reason.

$$Z_{app} = Z_{AB} + Z_{BF} + \underbrace{\frac{I_{PEID}}{I_A} \cdot Z_{BF}}_{\text{additional impedance}} \tag{5.2}$$

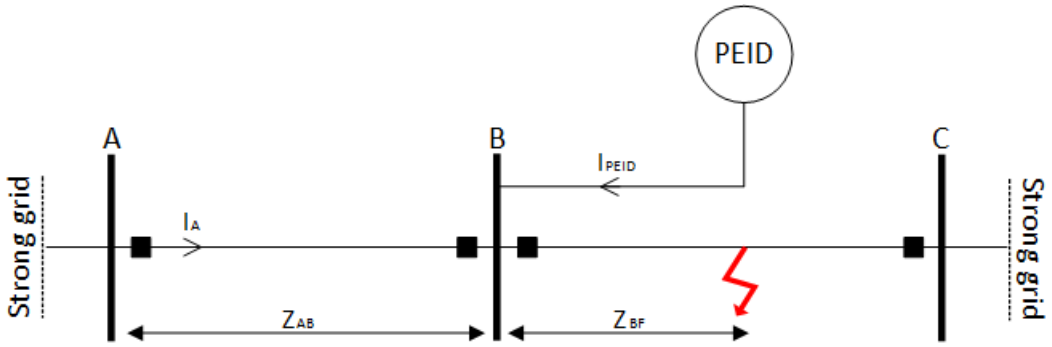

Figure 5.2: An example topology with intermediate infeed from PEID:s.

Another issue is related to voltage phase angle jumps previously mentioned in section 4.3.3, as some distance protection use memory-polarized voltage for doing impedance calculations. Memory-polarization refers to the usage of voltage measurements in the faulted phase a moment before fault inception. In conventional power systems, it can be assumed that the pre- and post fault voltage angle does not differ significantly, but this assumption may not be valid with the presence of PEID:s as the converter controller may be capable of cause voltage phase jumps. This can impact the impedance computation negatively [22].

5.2.2 Directional function

As previously stated, fault current injection by PEID:s may lack or contain only a small negative sequence component. Directional elements used in some distance protection deployed in the Swedish transmission grid uses the negative sequence current and voltage to determine fault direction. One advantage of this type of algorithm is that negative sequence components is not effected by mutual coupling [5] or load flows. Traditionally, this has been an effective algorithm as negative sequence current has been present in sufficient quantities during unbalanced faults, but this may not be the case in PEID dominated networks.

The questionnaire that was sent to protection manufactures as a part of this thesis project contained a question regarding how this algorithm work, as it is currently not known by Svk. One vendor confirmed that the algorithm uses the negative sequence current, but they were unable to disclose any further information about the algorithm due to confidentiality. Furthermore, this vendor indicated that the functionality was not threatened by PEID integration, as the the response contains negative sequence current prior to steady-state. Faults including resistance of 10 ohms or higher is expected to come with more challenges to directional functions according to this vendor.

Reference [21] on the other hand found that the inconsistent fault current injection during the transition period can lead to falsely declared direction. This was investigated with a detailed RTDS model of a 100% PEID network and HIL tests of distance protection from different vendors, but the specific directional algorithm was not disclosed. Issues posed by PEID fault current injection to directional algorithms is also raised in reference [22] as one of the biggest challenges for distance protection posed by PEID:s. This reference did not express risk of false direction clarification, but merely recognized that lack of negative sequence current will make negative sequence based criteria insufficient for protection purposes. Furthermore, reference

[19] discusses a directional negative sequence overcurrent element based on the angle between the negative sequence current and voltage. A forward fault normally causes the negative sequence current to lead the negative sequence voltage by 90° whereas it lags the negative sequence voltage by 90° for reverse faults. As mentioned in section 4.3.1, another angular relationship may occur in presence of PEID:s, which will impact the performance of this type of directional function negatively.

5.2.3 Fault identification logic

The fault identification (FID) logic or faulty phase selection algorithm, is a function used in distance protection in order to identify the fault loop, i.e. the type of fault and the faulted phase/phases. A common FID logic uses the phase angle between the negative- and zero sequence current for this purpose, based on a presumed mathematical relation between these quantities. This relation holds in SG dominated networks because of the inductive nature of the negative sequence network and machine impedance [18]. On the contrary, studies show that this relationship might not always be the case in networks with a significant presence of PEID:s, which lead to misoperation of this type of FID logic in presence of PEID:s. However, there are many other types of FID algorithms, and different vendors uses their own version.

As previously mentioned, PEID:s may not inject negative sequence current at all in steady-state, and in that case, the FID logic does not have a negative sequence current to base decisions on. According to reference [19], some FID logics uses voltage if the fault does not produces sufficient negative and zero sequence current, for example like the FID logic mentioned on page 54 in reference [27], which showed promising performance in presence of PEID:s in simulation tests. Reference [19] compares current based FID performance through simulations of networks supplied by either only SG:s, only type IV WTG:s under the German grid code or only type IV WTG:s suppressing negative sequence current. For a SLG fault, the negative sequence current phase angle with respect to the zero sequence current is equal in the SG network and the WTG network under the German grid code. The other WTG scenario on the other hand, measures a phase angle deviating 136 °from the SG network, leading to the wrong phase decision. Furthermore, in reference [7], the FID algorithms detects balanced faults for some unsymmetrical faults because the WTG injects only positive sequence current. This was investigated using recorded transmission data converted into COMTRADE format and real protection units. However, it is unknown what type of FID logic was investigated in this case.

Reference [18] mentions that even if some PEID:s are allowed to inject negative sequence current, it is not certain that it will lead the negative sequence voltage by 90 ° as in SG dominated networks. This is dependent on the converter controller. Reactive negative sequence current injection according to the German grid code [5] for example, is favorable for traditional FID logics. This is also proved by reference [20]. Moreover, reference [20] investigates two commercial distance protection with different FID algorithms in presence of PEID:s; one based on the angle between the negative and zero sequence current and another based on superimposed quantities. With negative sequence suppression, both protection IED:s showed tendencies to refuse or delay trips. With reactive negative sequence current injection, the performance of the former algorithm improved considerably, whereas the latter algorithm still was not able to correctly detect all fault. Especially following grounded faults. The study concludes by recommending a time delay of 30-50 ms of zone 1, in order for the FID logic to base its decisions on steady-state quantities. Another study

from to the same project noted that the transition period gave rise to the most problems, but that the initial transient supports correct FID operation [20].

5.2.4 Extra current criteria

Some distance protection are supervised by an overcurrent sub-function in order to prevent inadvertant operation [19, 5, 28]. This can be viewed as a starting function. It is known that current based elements are prone to missoperate in PEID dominated networks due to the current limit of PEID:s, hence, overcurrent supervision may cause distance protection to refuse operation during faults. Reference [19] suggests picking the minimum threshold value for transmission lines emanating from inverter-based resources and use back up undervoltage protection. This means that current and/or voltage must exceed a specified threshold. However, reference [28] concludes that according to their tests, distance protection performance is not increased with a minimum current threshold because other sub-functions fails to operate correctly. This study also mentions that decreasing the threshold may add the risk of false tripping as drops in voltage is not always a product of a fault. It could for example drop during switching of loads and capacitor banks. Using negative sequence current as a starting function in distance protection also occurs, but this method is not suited in PEID dominated networks either, as the fault current injected could consist of positive sequence current only.

5.2.5 Power swing protection

There are mainly two types of power swing protection elements: power swing blocking (PSB) and out-of-step tripping. The power swing blocking function works through measuring the rate of change of current and voltage and is able to distinguish between a power swing and a fault because the rate of change during the former is slow and the latter is fast. However, as PEID:s normally does not provide inertia to the system, it is likely that the rate of change during power swings will increase. This will make it more difficult for power swing blocking function to operate correctly [19]. During a discussion with a vendor, the large difference in time scales between faults and power swings was brought up in favor of the PSB function in PEID dominated networks, but the vendor concluded that this topic required more thought.

Out-of-step tripping is used to determine if a swing is stable or not. In the case of an unstable power swing, tripping may be initiated in order to decrease risk of widespread outages. Reference [19] shows that this function may missoperate under some PEID scenarios, classifying a stable swing as unstable, leading to unwanted tripping. The reference suggest changing the settings of the out-of-step tripping element based on the the most stable swing in PEID scenarios.

5.2.6 Multi criteria algorithm

Traditionally, protection algorithms work on the basis of decision trees, where one criteria at the time is analyzed and the result is locked before analysis of another criteria is initiated. This approach limits the possibility to use a combination of several functions to make decisions, which may be a way of mitigating misoperation caused by PEID:s [22]. Multi criteria algorithms on the other hand, makes decisions based on the agreement of several functions or use weighting or priority formulas in order to select the most accurate

one for specific grid conditions. It could be based on instantaneous current and voltage, incremental current and voltage, negative and zero sequence current and voltage, impedance computations, phase jump detection [20], memory- and cross polarized voltage etc. Depending on detected grid conditions, some criteria is excluded from the decision process. For example, if a transmission line sometimes (for example in a N-1 scenario) only interfaces negative sequence suppressing PEID:s, the multi criteria would give the negative sequence current criteria a low priority and use another function for the direcitonality decision. One commercial example is the the multi-criteria loop selector discussed during conference [22], which instead of using a decision tree approach, evaluates a weighted result from several functions in order to make directional, faulty phase, distance decisions etc. This approach is heavy in terms of data processing, but it enables the use of phasor-based protection functions in presence of PEID:s and works without communication to other protection units. Another proposed multi-criteria algorithm, based on instantaneous current and voltage, is briefly presented on page 46 in reference [27]. Lastly, multi criteria algorithms are used in some distance protection installed in the Swedish transmission system today, but it is not standard practice.

5.2.7 Communication schemes

Communication schemes can use different acceleration methods to initiate permissive signals to remote protection devices. If this method is based on functions that are in risk of misoperation in presence of PEID:s, the communication scheme also risks misoperation. For example the directional function previously discussed, which can depend on the negative sequence current and voltage. Reference [19] shows an example where an incorrect directional decision by a directional negative sequence overcurrent protection blocks a POTT scheme from sending a permissive trip signal to the remote protection unit. Furthermore, reference [5] discusses a real-life out of zone fault case, where a negative sequence directional polarization POTT scheme with echo logic fails due to interference by PEID:s. One protection unit, that interfaced a strong grid, sent a permissive trip signal to a remote protection unit after detecting a forward fault. The remote unit interfaced PEID:s and because this unit failed to detect a reverse fault, an echo pulse was sent back, allowing the first unit to trip fast for an out of zone fault. For ground fault protection, zero sequence voltage polarized directional protection IED is a better criteria utilized in POTT schemes [19, 5]. A solution for phase faults was not revealed.

As previously mentioned, communication schemes between distance protection at each line end is standard practice at Svk. Specifically PUTT and POTT schemes, but recently weak-infeed logic has been included if one line end is weak. A vendor consulted during this project mentioned this combination as a way of mitigating issues associated with PEID integration. However, the vendor underlined that this did not only apply to PEID:s, but to weak infeeds in general. This combination is also mentioned as an enabler in reference [29], but this reference too only refers to the inverter-based generation as a weak-source, and does not take into account previously described operation challenges of distance protection. There is a possibility that the acceleration methods used in protection produced by the vendor and discussed in reference [29] is not impacted by PEID:s. Regardless, an evaluation of used acceleration methods is recommended in cases where communication is used if PEID:s risk being the only fault current source.

5.3 Residual overcurrent protection

Studies on how PEID:s affect the specific type of ground overcurrent protection used by Svk has not been found in the literature, but there are studies on zero sequence overcurrent protection. This protection scheme is sometimes used as a synonym for the residual overcurrent protection, but small differences can occur. It is assumed that conclusions made about the former can be applied to the latter for this reason. First, reference [19, 5, 21, 17] recommends zero sequence overcurrent protection for ground protection in PEID networks, assuming that the PEID:s are connected through a transformer that is a zero sequence current source. In addition, this protection scheme will be predominantly independent of the type of PEID and its associated control algorithm [5] as it does not provide zero sequence current in itself. This is very favorable from a protection planning point of view as the range of possible fault responses from PEID:s are very large. In addition, settings of residual overcurrent protection is not impacted by load current, as load current can be assumed to be balanced at all times.

Step 1 and 2 of the residual overcurrent protection used by Svk is in general very sensitive to changes in grid topology, for instance if a transformer is disconnected temporarily. In addition, many working hours is needed in order to find the correct current level settings. If modern distance protection is installed on a transmission line today and is capable of detecting ground faults, step 1 and 2 of this residual overcurrent protection is deactivated in order to reduce the workload of protection engineers. As PEID:s impact several sub-functions of distance protection, it is not apparent if distance protection will be able to cover ground faults initially covered by step 1 and 2 any more. Step 23 and 3 are always activated however, as they can be used without changing settings when components are out of service and settings can set sensitively in order to detect high impedance faults.

Chapter 6

Other protection types suitable in presence of PEID:s

This chapter aims to summarize findings about protection schemes not yet deployed in the Swedish transmission system, that may be suitable in presence of PEID:s. The available research on this topic is limited however, as focus has been on investigating the performance of traditional protection schemes. Nevertheless, the aim of this chapter is to summarize findings relevant to objective iii, i.e. finding mitigation strategies to protection problems introduced by PEID integration.

6.1 Time-domain protection

Ultra fast protection schemes is an emerging research area partly because the replacement of SG:s with electrically decoupled RES will decrease the total inertia of the power system. Low inertia systems may reach instable conditions fast following disturbances, from where the system may not be able to recover from. In such systems, fast fault clearing is essential in order to prevent large-scale disturbances caused by faults such as short-circuits [30]. However, protection IED operating time is only a portion of the total fault clearing time, since modern circuit breakers has interrupting times between 30-40 ms [31]. As previously mentioned, Svk typically requires distance protection to operate within 25 ms.

Advancements in data acquisition and signal processing are two enablers for faster protection, which has made development of protection functions in the time-domain possible. These are capable of establishing phasor information in a short time. Significantly faster than 0.5-1 period (10-20 ms) of data acquisition, which is needed in traditional phasor-based measurements according to Svk. Two common protection types in the time-domain are incremental quantity and traveling wave (TW) based protection, which will be introduced in the following sub-sections. These have been mentioned in the literature as possible protection schemes for PEID penetrated systems [32, 28, 33]. All though the development of these protection schemes are justified mainly by the need of increasing stability in low inertia systems through lowering the fault clearing time, another advantage is that protection responding to transients are inherently less dependent on the sources and more dependent on the network itself. Hence, applications near PEID:s are possible [34].

6.1.1 Traveling wave protection and fault locators

TW:s are high-frequency (2 kHz-10 MHz) electromagnetic waves caused by disturbances in power systems, propagating approximately at the speed of light along overhead lines and cables. This is a phenomenon with a duration in the order of microseconds or maximum milliseconds [33]. TW protection is able to detect these transients in less than 1 ms using high-frequency measurements in the time-domain. Moreover, TW protection and fault locators does not depend on the fault current, which is a significant advantage for transmission lines emanating from PEID installations or highly PEID penetrated systems [30, 35, 33]. It is not dependent on the source impedance ratio either [33]. Other advantages with TW protection include not being dependent on fault type and fault resistance, as well as working well for compensated transmission lines. On the other hand, a significant disadvantage is that TW is produced only when disturbances does not occur at the voltage zero crossing. This means that TW based protection or fault locators cannot be used without back-up protection [30].

There are installed TW based devices today in some countries, but they are almost exclusively used for fault localization [33]. These devices can be categorized as single-ended or double-ended. The latter uses communication links between transmission line ends in order to locate faults based on the arrival time of TW:s on both sides [30]. Proper time synchronizing is crucial for this application, for example using Global Positioning System (GPS) [35]. Single-ended TW schemes does not rely on commutation, as it usually works through detecting the initial TW as well as the reflected wave locally. Theory on how TW:s are refracted and reflected when reaching a junction in the power system can be found in reference [30].

TW based protection schemes have been researched at transmission level for decades and several signal processing methods have been proposed in the literature, but amongst reviewed methods in reference [30] from May 2021, TW analysis through differentiator smoother filters is the only method used in protection available for commercial use. This protection scheme uses a TW differential and directional function in combination with incremental quantity based functions and a fiber-optic channel between measuring points, promising trip times between 1-5 ms. The differential function detects faults through comparing the wave polarity at the local and remote end of the line. A TW entering one side with a given polarity leaves the other line end with the opposite polarity for external faults, whereas TW:s generated by internal faults has the same polarity. This is illustrated in figure 6.1. Furthermore, the differential function utilizes the relative polarity of the current and voltage TW:s. The fault is forward if the TW:s are of opposite polarities and reverse if they have the same polarity [36]. This is visualized in figure 6.2. The TW line propagation time is a critical setting, which is best measured through a line energization test, but can be obtained from simulation using an electromagnetic transients program (EMTP) as well [36]. In contrast, settings of most traditional protection schemes can be made with steady-state simulations as input.

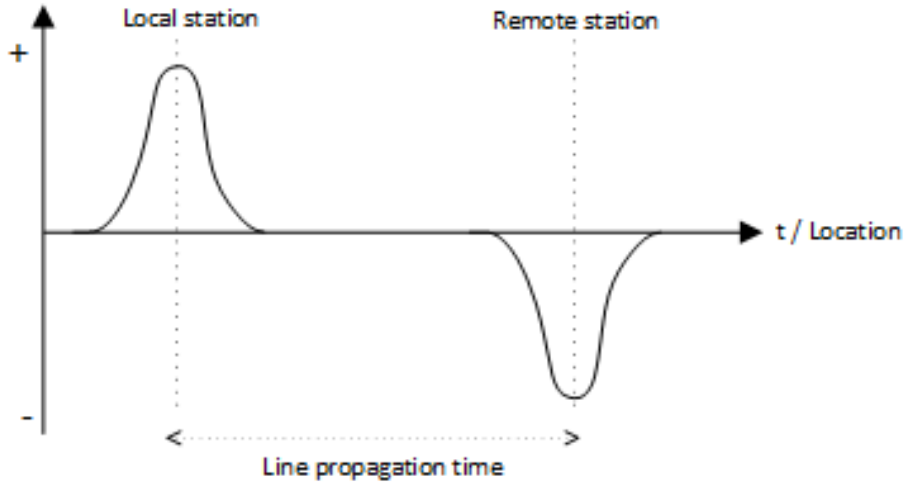

(a) External fault.

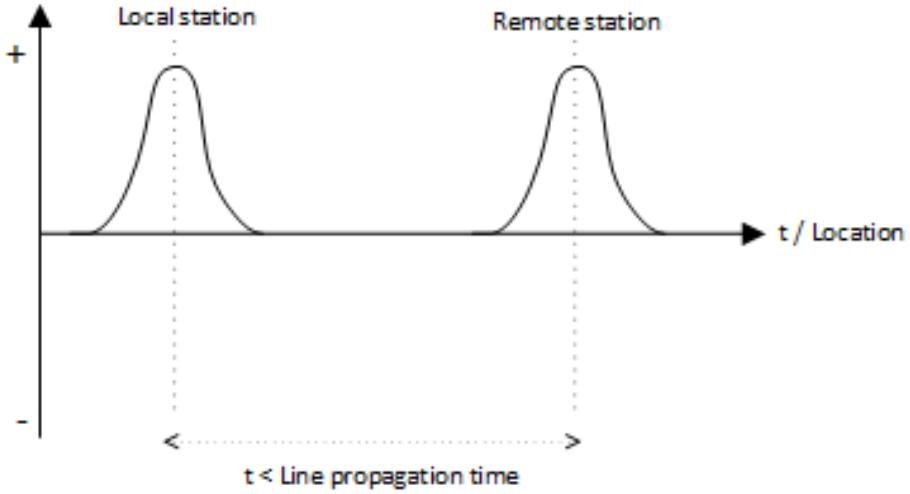

(b) Internal fault.

Figure 6.1: Polarity and timing of TW:s. Can be either current or voltage TW.

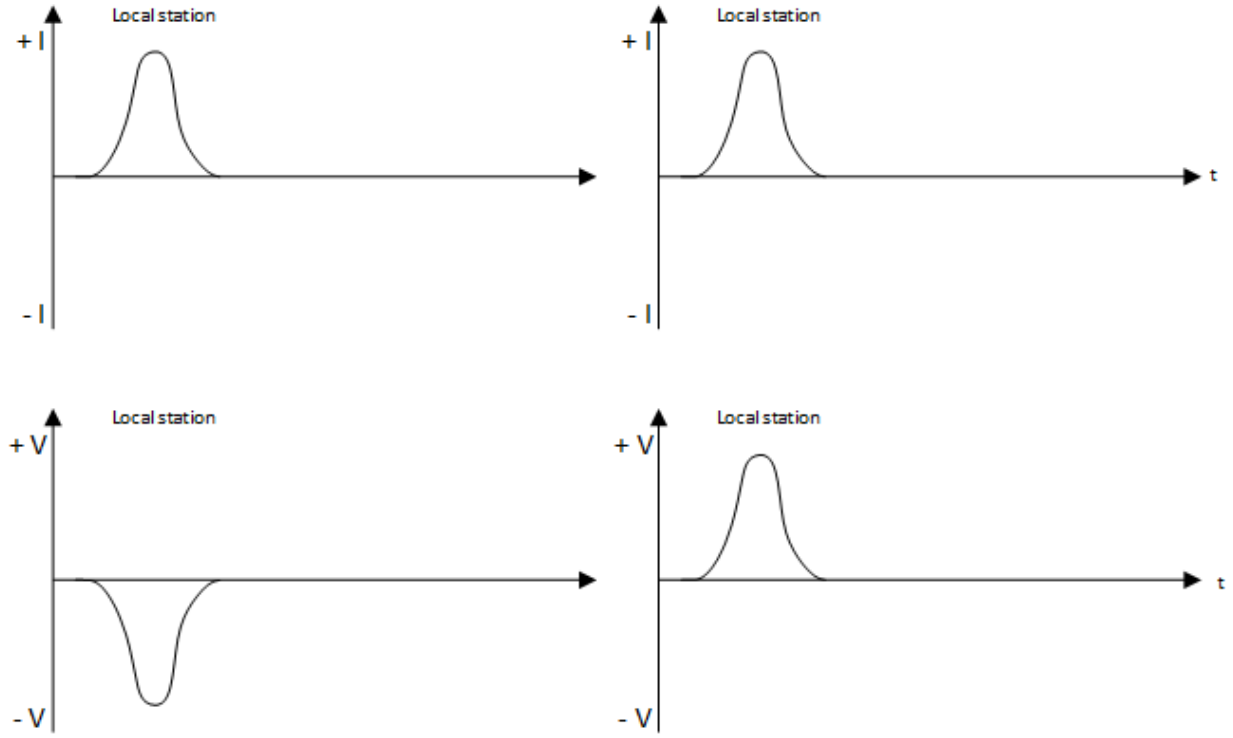

(a) Forward. (b) Reverse.

Figure 6.2: Direction determination based on current and voltage TW polarity.

6.1.2 Incremental quantity based protection

Incremental quantity based protection, also referred to as delta quantity and superimposed quantity based protection, utilizes the difference between pre- and post-fault instantaneous voltages and currents, hence, it consist only of the fault-induced portion of the electrical quantity. This can be described by equation 6.1, where ΔS is the incremental quantity, S is the measured instantaneous value, p is the number of cycles, t is time and T is the period of the measured quantity [34]. Normally, these properties are calculated with a rate between 5–10 kHz and the instantaneous values is saved for one cycle [36]. The advantage of these time-domain algorithms is mainly the high speed decisions possible, compared to traditional phasor-based protection schemes.

$$\Delta S(t) = S(t) - S(t - pT) \tag{6.1}$$

This technique has been used for fast-operating faulty phase and directional algorithms before, some utilizing the fact that the incremental voltage phasor is equal in phase and magnitude to the product of the incremental current and the negative incremental source impedance behind the protection unit [37]. Reference [37] shows that traditional incremental property based protection risk malfunction due to inconsistencies in the PEID response during the transition period. To overcome these issues, an adaptive window is introduced

that allows directional and faulty phase selection to occur during the initial transient. This algorithm is implemented in a multi-criteria algorithm, shortly presented in section 5.2.6.

6.2 Adaptive protection

Adaptive protection is mentioned in the literature as a possible solution for meeting protection requirements in systems with variable grid operating conditions [38, 25, 39, 32, 40]. Any changes in settings of conventional protection schemes has to be executed on-site. Adaptive protection schemes on the other hand, work on the premises of adjusting protection settings and characteristics automatically in response to changes in operating conditions of the power system. It can be applied to a single protection unit (adaptive relaying) or be integrated in a wide-area monitoring, protection, and control (WAMPAC) system [39], which can be used to counteract the propagation of large disturbances. According to reference [32], the following actions can be included in adaptive protection schemes used to mitigate issues caused by variable RES protection and grid topology changes.

1. Capture the current PEID output level.
2. Capture current protection settings.
3. Update the model according to 1 and 2.
4. Perform a protection security assessment using the model.
5. Evaluate suitable settings based on result from 4 and the utility protection philosophy.
6. Deploy settings in real protection unit.

Reference [41] presents an adaptive solution for remote infeed from PEID:s. Recall the topology displayed in figure 5.2 and equation 5.2, showing that the apparent impedance seen at position A varies depending on the level of infeed from PEID:s. The proposed adaptive distance protection scheme uses the measured infeed current and voltage measured at the remote bus (bus B) to automatically update the zone 2 and 3 reach setting of distance protection at position A. This is done using a radial basis function neural network, considering different fault resistances and in this way, attuning to prevailing system conditions. The need of such adaptive protection schemes is dependent on the capacity of variable infeed though, as small capacities impacts the impedance measured at bus A less than large capacities.

Reference [25] instead focuses on solving the issue of inconsistent impedance measurements described by equation 5.1, caused by the limited current amplitude of injected current I_A by converters and the phase angle difference between this current and the total fault current (I_F). An adaptive algorithm is proposed, which computes the line impedance from the distance protection to the fault point (Z_{AF} in figure 9.1) by computing the angle between I_A and I_F (α) using local measurements only. Therefore, I_F is not available as it depends on the infeed from the remote line end. Instead pure-fault sequence networks of the PEID for different fault types is derived using incremental properties, which can be used to obtain α. An advantage about this proposed algorithm is that is does not need information from other measuring points.

Several other adaptive distance protection is proposed in the literature [42, 43, 44], some in need of information from remote measuring points and others rely on local measurements, like the one previously presented. A protection vendor consulted within this thesis project mentioned adaptive distance relaying based on source impedance, however, this was merely mentioned in discussions and no specific algorithm was revealed. Moreover, adaptive differential protection is mentioned as a key research area in reference [24], specifically adaptive settings of restrain current level depending on operation mode of the power grid. This due misoperation risks associated with solar parks connected to weak power systems and the impact of phase angle of injected current.

For any type of adaptive protection, the time needed to change a setting or a setting group is a critical operating characteristic of adaptive protection according to reference [45]. In addition, communication time, communication dependence and in some cases time synchronization are examples of other less favorable aspects relating to adaptive protection. Furthermore, from reviewed information in this thesis project, no adaptive protection schemes has been found commercially available. However, a pilot implementation has been deployed in Germany according to reference [32].

Chapter 7

Steady-state short circuit model

This chapter introduces the short circuit program used in this thesis and presents the short circuit models used. These models represents the short circuit network exclusively and does not include loads. The purpose of the two models produced for this thesis is to investigate the performance of protection on a transmission line connecting PEID:s radially (Sub-grid 1a and 1b) and in a high PEID penetration scenario (Sub-grid 2).

7.1 General

Steady-state short-circuit calculations are a procedure commonly used by system operators for protection coordination and setting. PSS®CAPE is a steady-state short circuit program used by protection engineers at Svk. Specifically the short circuit module in PSS®CAPE. In this thesis project, Svk:s base model of the current power grid in Sweden is used and adjusted to support investigations made within the project. This model includes almost every station, transmission line, cable and generator in the 220 kV and 400 kV transmission system. It also includes the sub-transmission network, as well as short circuit and ground-fault current contributions from other countries in the same synchronous area as Sweden. The model does not include loads as it is only used for short-circuit and ground-fault calculations.

7.2 The type IV WTG model

The type IV WTG model used in this project was obtained from PSS®CAPE:s library of generators and it is validated against EMTP simulations by the model developer in reference [17]. No further validations tests has been performed by Svk. Furthermore, it models aggregated wind turbines with a single LV-MV transformer and a filter in parallel. The type IV model essentially models the parts included in the basic type IV WTG configuration displayed in figure 4.3b, with the additional filter. This model can also be used to model VSC-based solar power and HVDC links.

The model uses an iterative method based on steady state equations to calculate the fault current injected by the the WTG:s two cycles after fault inception. Therefore, a solution is not always found. Within the thesis project however, some recurrent iteration issues occurred, for example when numerous WTG:s was

connected to the model simultaneously. This limited some investigations in the thesis project. A further description of this model and its algorithm can be found in reference [46] and in [17]. If not otherwise stated in the report, the iteration tolerance and maximum iteration was set to 0.01 and 30.

Dynamic reactive current injection (control mode FRT) with reactive power (Q) priority is used in this project. This is a common control mode, which aims to support the voltage at the LV node by injecting or consuming reactive power. Q priority entails that if current limits are reached, the needed or the maximum (with respect to current limits) reactive current will be injected, whereas only portions or zero active current is allowed.

Table 7.1 displays the model settings used in this project. Here, the current limit refers to the maximum allowed output current and k is the rate of change of reactive current proportional to the voltage drop at the LV. Deadband refers to an interval of voltage where additional reactive current is not injected, i.e. during faults of low severity or faults far away from the converter. These are common control settings and the default values of the model. The transformer resistance (R) and reactance (X) are average values based on data obtained from a selection of real wind parks in Sweden. These wind parks are modelled in PSS®CAPE in this thesis project, which is further described in section 7.3. Furthermore, the short circuit power contribution of the filter admittance is small in relation to the contribution from the converter and is therefore neglected.

Table 7.1: WTG model settings in p.u. on generator base.

Parameter	**Value [p.u.]**
Current limit	1.1
k	2
Deadband	0.9-1.1
Transformer R	0.005
Transformer X	0.08
Filter G	0
Filter B	0

Another control mode used in this project is constant power factor (PF) with P priority. As opposed to Q priority, P priority injects the needed or the maximum (with respect to current limits) active current if current limits are reached, whereas only portions or zero reactive current is allowed. With this control mode, a desired PF is chosen, which is defined as PF = $\cos(\theta)$ and the corresponding reactive current production/consumption is defined by Q = P·tan(θ). In PSS®CAPE, PF ranges between -1 and 1. If entered as a positive number, the angle θ ranges between 0 °and 90 °, and the converter therefore produces reactive power if P is positive. On the other hand if it is entered as negative number, θ ranges between -90 °and 0 °, and the converter consumes reactive power if P is positive [46].

7.3 Sub-grid 1a - An existing wind park

Sub-grid 1a can be seen in figure 7.1 and it represents an existing collection of wind parks, associated distribution grid and the nearest parts of the transmission system. However, the model also includes the rest of Svk:s base short-circuit model described earlier, but this is not shown in the figure. This sub-grid will be used to investigate potential protection challenges due to PEID:s that may already occur in the Swedish transmission system, as wind park connections similar to this one already are present.

Everything in the model except for the WTG:s and LV-MV transformer was modelled by Svk previous to this thesis project. Data on LV-MV transformer impedances and wind power capacity was also provided and used to complete the sub-grid model. Each WTG in the figure is equivalent to several wind turbines/one wind park and each WTG is assumed to be of type IV. The total capacity amounts to 847.5 MVA and the different colors in figure 7.3 shows associated voltage levels of the sub-grid. Violet, blue, green and orange represents 400 kV, 135 kV, 33 kV and 0,575 kV.

Due to convergence issues associated with the used type IV WTG model, two SG:s are also included in the model, with the following positive, negative and zero sequence impedances: 6.589, 14.0056 and 14.0056 ohm. These SG:s provides a small fraction of the total fault current and are therefore assumed not to interfere with simulation results. It is assumed that all WTG:s are of type IV and standard control settings presented in table 7.1 are used. Furthermore, line parameters of the line between station A and B (line AB) is used within this project, and these are presented in table 7.2.

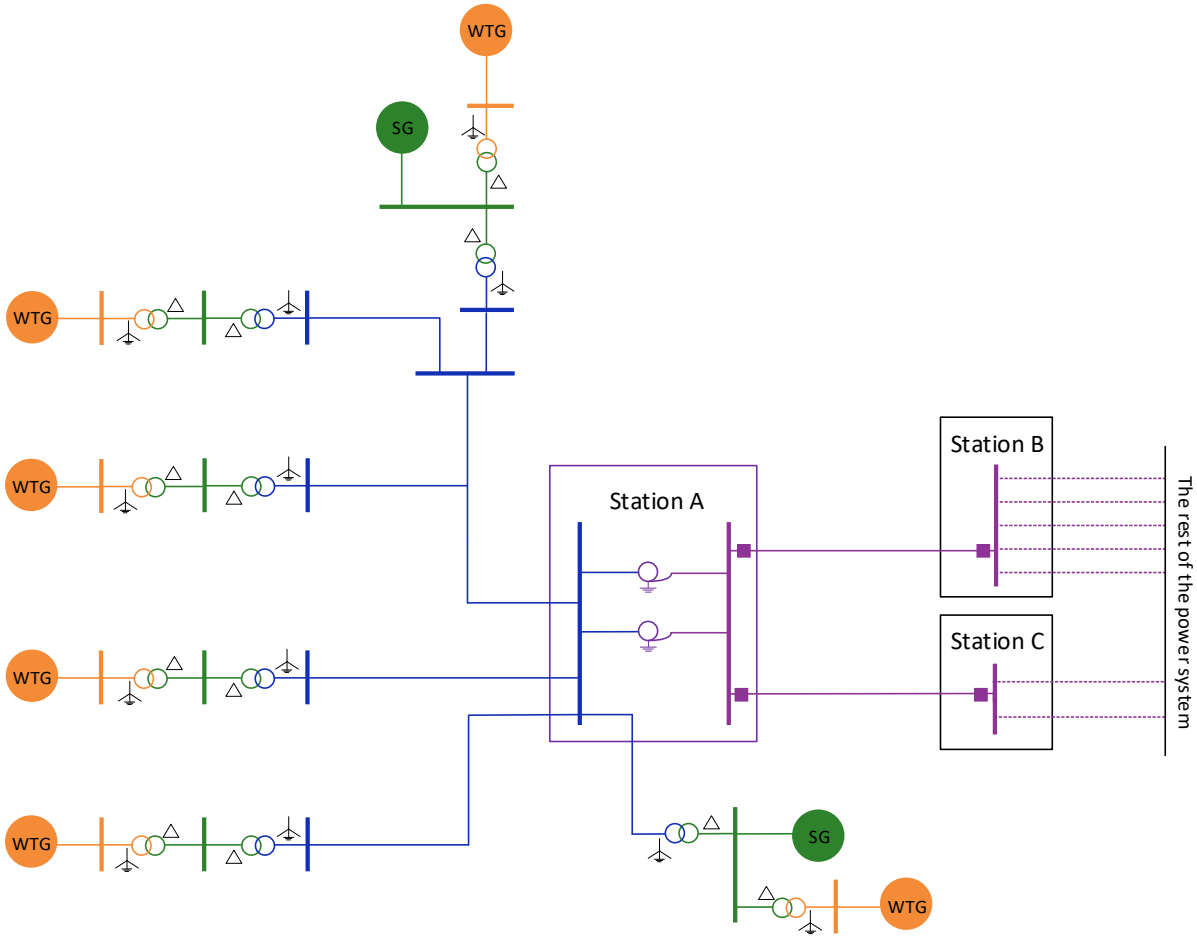

Figure 7.1: An illustration of relevant parts of sub-grid 1a.

Table 7.2: Impedance of line AB.

	R [ohm]	X [ohm]
Positive sequence	1.85	25.1
Zero sequence	19.0	64.6

7.4 Sub-grid 1b - A simplified wind park model

Sub-grid 1b is a very simplified version of sub-grid 1a. It can be seen in figure 7.2 that a generator is connected directly to the 400 kV bus, which would never occur in real life. The generator models aggregated wind power with a capacity of 847.5 MVA. This model was used because the WTG model experienced convergence problems when PF control mode was used, which was needed to perform the investigations

presented in section 8.2.1. Since there would be a significant zero sequence contribution from transformers in a real situation during grounded faults, only un-grounded LL faults were applied when this model was used.

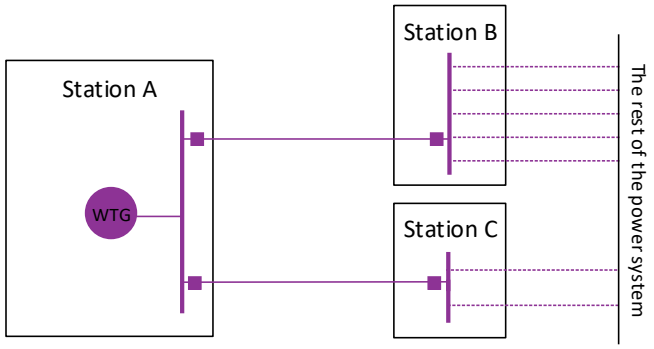

Figure 7.2: An illustration of relevant parts of sub-grid 1b.

7.5 Sub-grid 2 - A high PEID penetration scenario

Sub-grid 2 is used to investigate protection performance in a portion of the Swedish transmission grid in a future scenario. This model is loosely based on the scenario *large-scale renewable* for the year of 2045 in SE4, which is presented in section 4.1. This is one out of four scenarios presented in the long-term market analysis published by Svk in 2021, where all nuclear power plants in Sweden are shut down and the capacity of wind- and solar power increases considerably by the year of 2045 compared to present capacities. Therefore, a large capacity of type IV WTG is added and all nuclear power plants (Ringhals, Forsmark and Oskarshamn) and their associated transformers are discounted from Svk:s main short circuit model. A simplification made is assuming that the capacity of thermal power is not changed between the years of 2020-2025.The resulting model can be seen in figure 7.3, where the added renewable energy sources are marked with RES. Similarly to the previous models, Svk:s entire short circuit model is included but not shown in the figure. More over, RES is not connected to every station. The colors violet, blue, green and orange in the figure represents 400 kV, 135 kV, 33 kV and 0,575 kV.

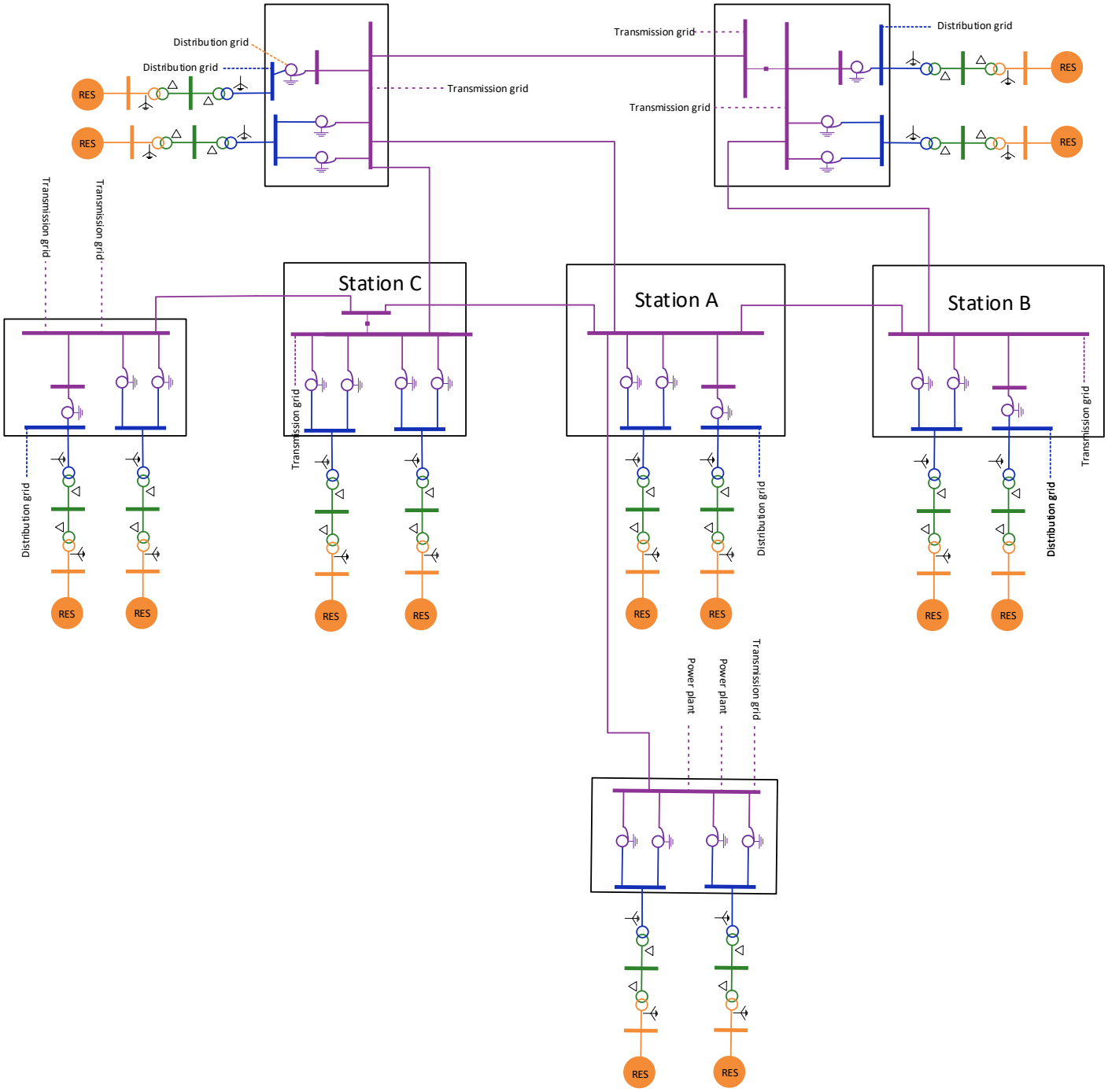

Figure 7.3: An illustration of relevant parts of sub-grid 2.

It is assumed that the connection points of all wind- and solar power is equally distributed between stations in the area, however, RES is only connected to six stations in the model because convergence issues occurred when a large capacity of WTG models were connected to the model initially. This is not believed to impact the result considerably as investigations in the thesis focused on the line between station A and B, and because WTG:s far away from a fault barely contributes to the fault current. Furthermore, 2/3 of wind power is assumed to be connected to the 400 kV transmission grid and 1/3 is assumed to the underlying distribution network respectively. Based on the fact that 10% of newly installed solar power was centralized in 2019, the amount of solar energy connected to a minimum voltage level of 135 kV is assumed to be 20% of the total capacity. Half is assumed to be connected to the underlying distribution network and half to the 400 kV transmission system in the model. In total, 965 MW wind- and solar power is connected directly to the 400 kV bus of each station and 510 MW is connected to each station via the underlying distribution grid. This is loosely based on SE4 specific capacities produced in the long-term market analysis by Svk, but they are not published in the report [2].

Each connected RES in the model is assumed to represent a collection of type IV wind parks similar to sub-grid 1a, meaning that the capacity is assumed to be distributed in smaller parks with their own park transformer and associated transmission lines. In order to simplify, the RES capacity of each station in the future model was aggregated using only one generator model, and the impedance of one delta-wye 34 kV-135 kV transformer was tuned to be equivalent to the network below 150 kV and above 34 kV in sub-grid 1a. As previously explained in section 7.2, the 0.575/34 transformer is a part of the type IV WTG model. Transmission lines and auto-transformers are copied from sub-grid 1, which were modelled by Svk previous to this thesis project. The portion of RES connected via the underlying distribution grid is connected to the transmission system via 150/400 kV transformers which is a part of Svk:s main short circuit model. Some stations does not have a distribution grid connection, and in those cases, the RES is connected via two auto-transformers as in sub-grid 1a. The same method is used for RES assumed to be integrated directly to the transmission system.

Chapter 8

Simulation results

This chapter presents the computational result based on simulations conducted in PSS®CAPE and aims to provide answers to objective ii, i.e. how conventional protection is impacted by PEID fault current injection. The chapter will investigate how different grid topologies and pre-fault active power references affects the voltage measured and the impedance computed by distance protection. The operation of line differential protection is also investigated depending on the phase angle of injected current by the PEID:s as well as the strength of the grid side. One of the investigated sub-grids is the connection point of a collection of wind parks in normal operation and in a N-1 scenario, where the wind parks are connected radially. The other investigated sub-grid is a potential future grid topology where the penetration of PEID:s is high.

Henceforth, faults may be referred to in short, where SLG10 refers to a single-line-to-ground fault with 10 ohm resistance, SLG20 refers to a single-line-to-ground fault with 20 ohm resistance, and so on. As previously mentioned, 0, 10 and 20 ohms are used because it covers most earth faults occurring on overhead lines with ground wires, according to Svk:s experience. Moreover, in this chapter, P refers to the pre-fault active power production by the WTG:s, which is either 10% or 100% of the nominal power output. These scenarios are referred to as P10 and P100 hereafter.

8.1 Sub-grid 1a

This section investigates protection located on a transmission line emanating from a sub-station that connects a collection of wind parks. Normal operation refers to the grid topology displayed in figure 7.1 and N-1 refers to a scenario where the line between station A and C is out of service, hence, the wind power park is the only fault current source behind station A.

8.1.1 Impact of varying pre-fault power reference, fault resistance and fault location on the computed impedance

Figure 8.1 and 8.2 displays the impedance computed based on measurements at station A as a result of SLG faults, located in the middle of line AB and on the 400 kV bus at station B respectively. The impedance is

based on the line parameters in table 7.2 and current and voltage values obtained from simulations, and it is computed using equation 3.2 and 3.3. As previously mentioned, the method of computing the impedance may vary between protection manufacturers and year of manufacturing, therefore, the result may not hold for all types of distance protection.

The reach shown in the figures only represents the reactive reach of the distance protection, typically 85% and 120% of the positive sequence line impedance for zone 1 and 2 respectively. The resistive reach is usually more site specific and is therefore not shown in the figure.

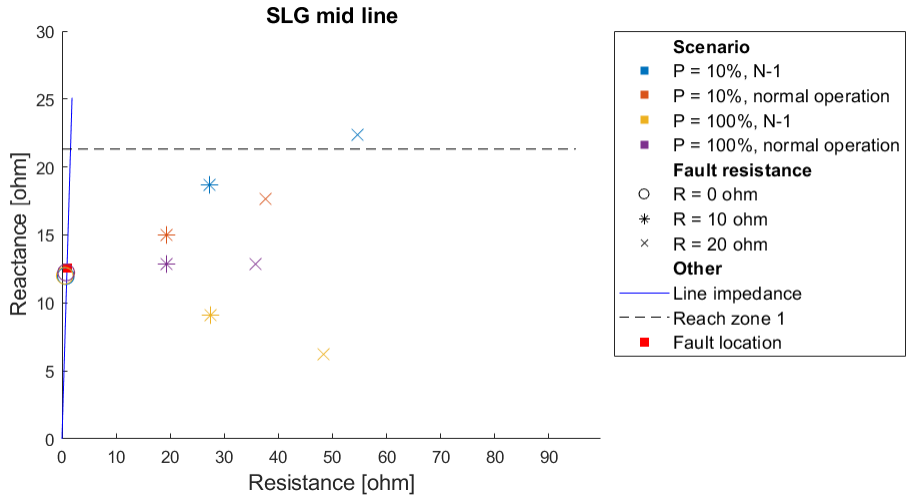

Figure 8.1: Impedance computed at station A, for midline SLG faults with different fault resistance.

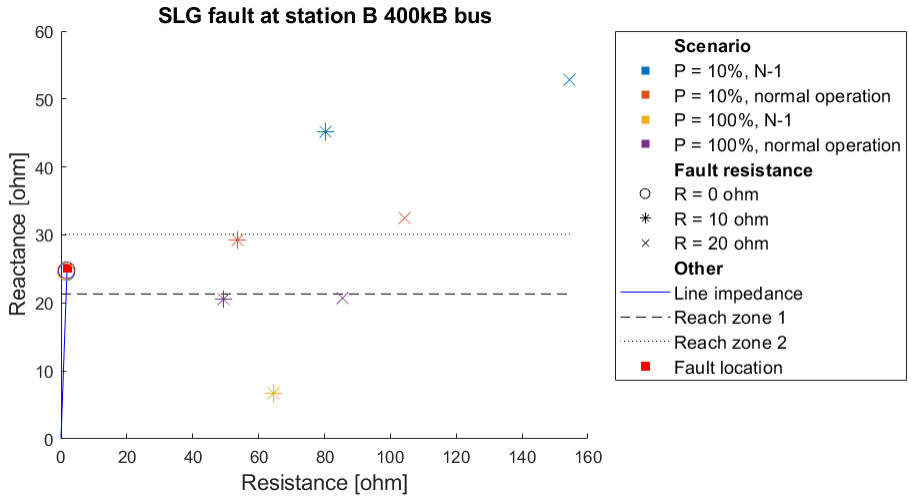

Figure 8.2: Impedance computed at station A, for SLG faults at station B with different fault resistance. The N-1 SLG20 solution did not converge.

According to the result, the pre-fault active power reference has a significant impact on the reactance computed by distance protection. For all high resistance faults, the apparent impedance consists of a smaller reactive component during P100 compared to P10. For example, in the mid line N-1 R=10 ohms case (blue and yellow *), the difference in reactance is around 10 ohms. This is caused by the fact that the fault current supplied by the PEID:s differs in both magnitude and phase angle depending on the pre-fault active power reference, and this can be explained using equation 5.1. Further explanation is provided for two LL faults further down.

Through comparing figure 8.1 and 8.2, it is also clear that the difference in reactance between P100 and P10 is larger when the fault is located at station B. However, the distance protection show over- and underreach tendencies on both fault locations. According to the result, the distance protection is more likely to underreach if the pre-fault active power production is low. In scenarios where the pre-fault active power reference is at nominal levels on the other hand, it tends to overreach.

As mentioned in section 7.2, the WTG injected current obtained from PSS®CAPE is the steady-state current two cycles after fault inception. In general, zone 1 distance protection trips faster than that, and therefore, it is likely that zone 1 would not trip based on the behaviour shown in figure 8.1. However, it is included in the report because some zones are time delayed and all zones of some older distance protection have longer operating times.

Figure 8.3 and 8.4 displays the impedance computed as a result of LL faults, located in the middle of line AB and at station B respectively. Equation 3.1 and simulated current and voltage obtained in PSS®CAPE are used to compute the impedance. The fault resistance applied in each LL case can be found in table 8.1, calculated using Warringtons formula presented in equation 2.1. The arc length of 11 m is used and for zone 2 faults, the length is assumed to be three times as long.

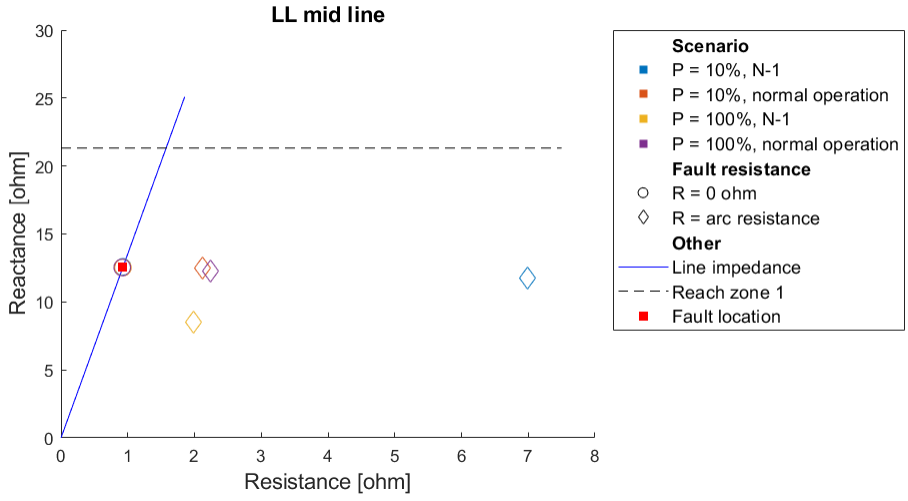

Figure 8.3: Impedance measured at station A, for midline LL fault. The arc resistances used are presented in table 8.1.

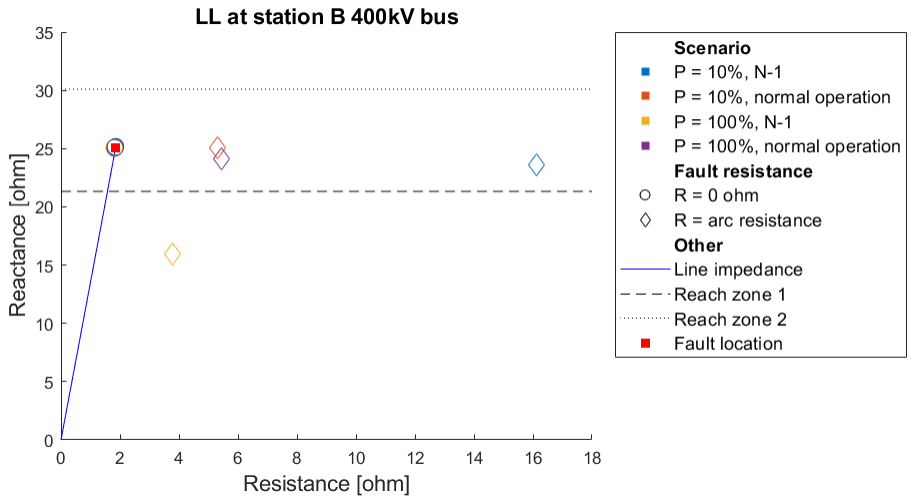

Figure 8.4: Impedance measured at station A, for LL faults at station B. The arc resistances used are presented in table 8.1.

Table 8.1: Arc resistance used in LL fault simulations.

Case	Fault location	Resistance [ohm]
P=10%, N-1	Midline	0.86
P=10%, normal operation	Midline	0.63
P=100%, N-1	Midline	0.92
P=100%, normal operation	Midline	0.66
P=10%, N-1	Station B	0.93
P=10%, normal operation	Station B	0.82
P=100%, N-1	Station B	0.96
P=100%, normal operation	Station B	0.84

Equation 8.1 is a version of equation 5.1 for line to line faults. It can be seen that the ratio of the total fault current (I_F) and the current measured at station A (I_A) dictates the phase angle of the additional impedance. Index b and c refers to phase b and c. Moreover, R_F is the fault resistance and Z_{AF} is the positive sequence line impedance from station A to the fault. If I_F and I_A are close in phase, the additional impedance will be predominantly resistive. On the other hand, if there are significant phase angle differences, the additional impedance will have a reactive component as well. The magnitude differences also plays a role in the size of the additional impedance.

Table 8.2 contains the total fault current and the PEID supplied fault current for two scenarios, both N-1 scenarios, with different pre-fault active power production. The impedance estimated by the protection at station A for these fault can be seen in figure 8.4, marked using yellow and blue diamonds. It can be seen that the apparent impedance differ significantly. In table 8.2, it is clear that the fault current in phase B is similar in both cases, whereas the PEID injected current differ significantly between cases. Hence, depending on

the topology and pre-fault power reference, I_A will have different characteristics, and therefore, the apparent impedance will vary.

$$Z_{app} = \frac{V_{Ab} - V_{Ac}}{I_{Ab} - I_{Ac}} = Z_{AF} + \underbrace{\frac{I_{Fb} - I_{Fc}}{I_{Ab} - I_{Ac}} \cdot R_F}_{\text{additional impedance}} \tag{8.1}$$

Table 8.2: Total fault current and PEID injected current for faults at station B, including arc resistance.

	P10, N-1	**P100, N-1**
I_{Fb}	19510.6 $\angle -172.3$ °	19020.7 $\angle -169.6$ °
I_{Ab}	702.668 $\angle 170.5$ °	1205.43 $\angle -118.7$ °

8.1.2 Secundary voltage levels with varying line length

Figure 8.5 displays secundary voltage at station A as a function of line length, for different fault types at station B, with different pre-fault active power references. Additionally, the voltage in normal operation is presented with dashed lines and N-1 with full lines. Voltage levels after a fault is a measure of source strength and is relevant from a protection perspective because measuring accuracy of protection will degrade if the voltage falls too low. According to reference [47], in general, protection need at least 5 V. However, some manufactures requires less, for example more than 3 V.

In figure 8.5b, both phase B and C is shown for LL and LLG faults, as their voltage differ significantly. In the other cases, the voltage is equal in all faulted phases.

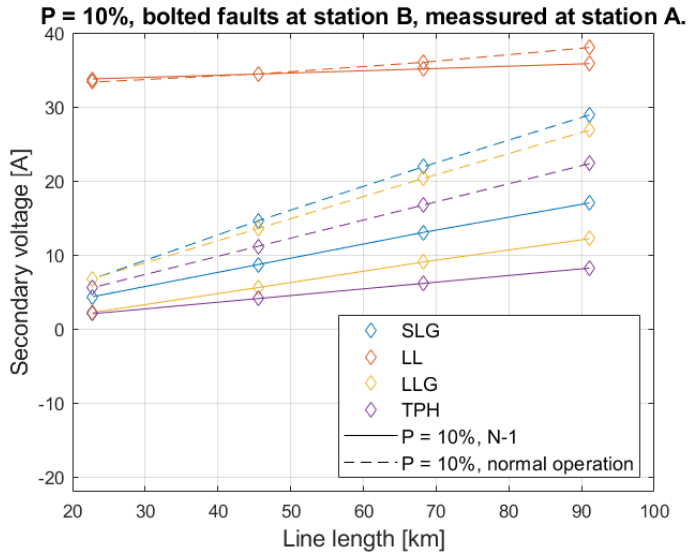

(a) P = 10%.

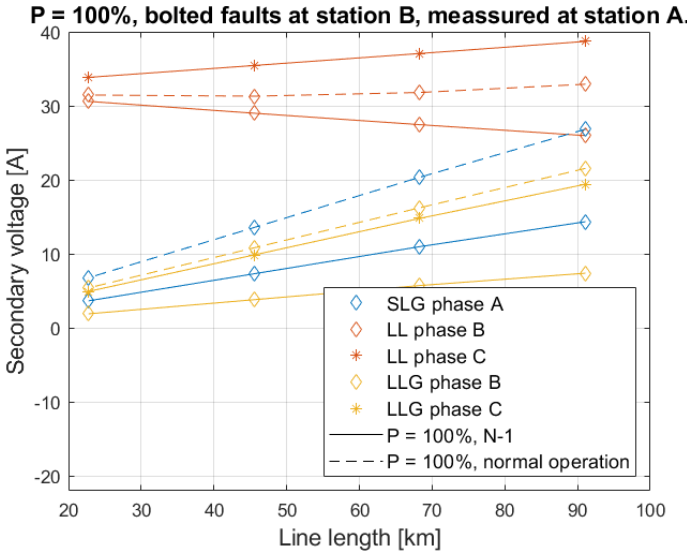

(b) P = 100%. TPH did not converge.

Figure 8.5: Voltage at station A as a function of line length, for bolted faults at station B.

It can be seen in both sub-figures that the secundary voltage risk falling below 5 V for short transmission lines after bolted TPH, LLG and SLG faults. In such cases, non-voltage dependent protection should be used, for example line differential protection, if current levels are above accuracy limits of current measuring devices. Svk normally uses line differential protection for overhead lines < 25 km, but this result shows that it may be needed for longer lines as well if PEID:s risk being integrated radially. Moreover, the voltage following LL faults does not fall too low independently of pre-fault active power reference and if line AC is out of service or not. In P10, the N-1 scenario is clearly less strong than in normal operation. As the order of strength for each fault type is the same in both cases, e.i. TPG < LLG < SLG < LL, the P10 case can be

treated as a weak traditional short circuit source in this regard. The P100 case on the other hand, shows a new behaviour.

First, there is a large voltage difference between phase B and C for LL and LLG faults. In the LL case, the voltage even decreases with increasing line length, which is non-typical in traditional power systems. The reason for this behaviour could be the lack of negative sequence current or excess resistive positive sequence current, but detailed analysis is not performed in this thesis as the purpose of this investigation is to investigate the risk of measuring inaccuracies. Nevertheless, this indicates that a radially connected wind park cannot be equated with a weak SG sources in all operation modes.

As mentioned in section 7.3, the total wind power capacity in the used model is very large. The risk of not being able to support the voltage and therefore jeopardizing measuring accuracy will be greater for smaller parks. Especially for short circuit. Hence, protection engineers has to be vigilant when planning protection for small wind parks if they are connected via shorter lines and if there is a risk of the park being connected radially at times.

8.2 Sub-grid 1b

8.2.1 Impact of grid strength and fault current phase angle on line differential protection

This section seeks to investigate how the performance of line differential protection is affected by the phase angle of the fault current. As previously mentioned in section 4.3.1, the phase angle of the current injected by PEID:s can vary between -90°and 90°in reference to the voltage. The model used for this enquiry is presented in figure 7.2, which is a very simplified version of sub-grid 1a. Due to limitations in the used WTG model, the generator was connected directly to the 400 kV bus at station A, in order to enable WTG control settings of different power factors. Therefore, only LL faults was included in this section since the zero sequence current contribution from the transformers would have a significant impact on the measured current. It is likely that the impact of different phase angles on line differential protection would be less for SLG faults, as the zero sequence current provided by the transformers constitutes a significant part of the fault current for grounded faults.

Figure 8.6 presents the result, accompanied by a commonly used line differential chart. Equation 3.4 and 3.5 are used, but other equations might be used by different protection vendors. The triangles displays computed differential and restrain current in a scenario where station B interfaces a strong grid. The squares instead shows the same result when only one transmission line (in addition to line AB) is connected to station B, making it interface a much weaker source. The same capacity of wind power is connected to station A in both cases. Through this investigation, power factor control mode is used in order to vary the power factor set point of the WTG. The power factor definition used by the WTG model can be found in section 7.2 or in reference [46].

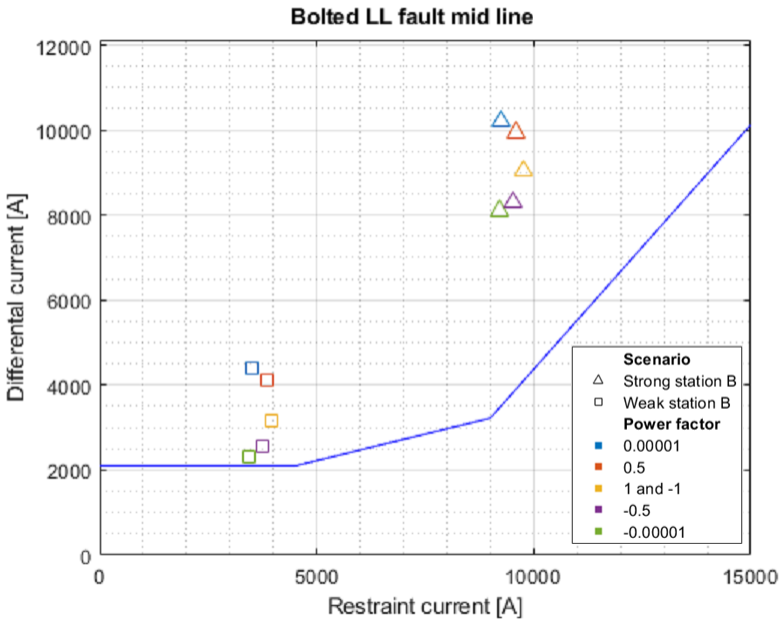

Figure 8.6: Differential and restrain current as a function of various power factors.

The result shows that the differential current may differ up to about 2000A for LL faults, depending on the power factor set point. However, as the aim of the converter control logic during faults often is to support the voltage and most type of faults causes voltage drops, $0 < PF < 1$ (i.e. current phase angle between 0 °and +90 °) is more likely to occur as it corresponds to reactive power production by the PEID. Therefore, a more likely differential current variation is 1000 A. Moreover, the result indicates that this is not a problem if the source behind the neighboring station to radially connected PEID:s is strong. If the source behind the neighbouring station is weak on the other hand, protection engineers may have to take this differential current variation into consideration when deciding on protection settings. In fact, differential protection may not be suitable for lines connecting two weak ends independently of power factor, if the line differential chart is not adjusted.

In reference to the presented rule of thumb in section 5.1, which states that line differential protection will operate correctly if the phase current on one side is 9 times larger than the other side. In this case the phase current at the station B line end is between 7.0-7.6 times than the current coming from the other line end, when station B is strong. On the other hand, when station B is weak, that line end supplies between 2.3-2.9 times more current compared to the line end connecting to station A. Hence, smaller differences between the phase current on both sides, compared to the rule of thumb, were possible in this topology and with this line differential chart.

8.3 Sub-grid 2

This section seeks to compare protection performance today and in a possible future scenario. The methodology is explained in section 7.5, including figure 7.3 displaying the future model. As previously mentioned,

the future scenario is only one of many possible future scenarios. The chosen one is interesting for this thesis project because the penetration of wind- and solar power is very high, at the same time as all nuclear power is decommissioned, reducing the short circuit power provided by SG:s in the system. During these simulations, the tolerance and maximum iteration was changed to 0.1 and 40 respectively, in order to facilitate a solution of the iterative WTG model algorithm. Lastly, it should be mentioned that only normal operation is considered in this section. Many simultaneous outages would impact the result.

8.3.1 Impact of varying fault resistance and fault location on the computed impedance

Figure 8.7-8.12 displays the impedance computed as a result of SLG and LL faults, located in the middle of line AB and on the 400 kV bus at station A and B respectively. Equation 3.1 is used, based on line parameters in table 7.2 as well as current and voltage phasors obtained from simulations. Table 8.3 presents arc resistances used for LL faults, calculated using Warringtons formula and the arc length of L = 11 m. For zone 2 faults, the length is assumed to be three times as long.

Figure 8.7 displays results for SLG faults with varying fault resistance, located in the middle of line AB. The impedance is measured on both sides of the line and is presented in separate subfigures. This is done for LL faults as well, presented in figure 8.8. Moreover, figure 8.9 and 8.10 shows impedance computations for faults at station B, that are computed using measurements at station A. This is an example of a zone 2 fault. The opposite is displayed in figure 8.11 and 8.12, where faults are applied at station A, and computed by protection located at station B.

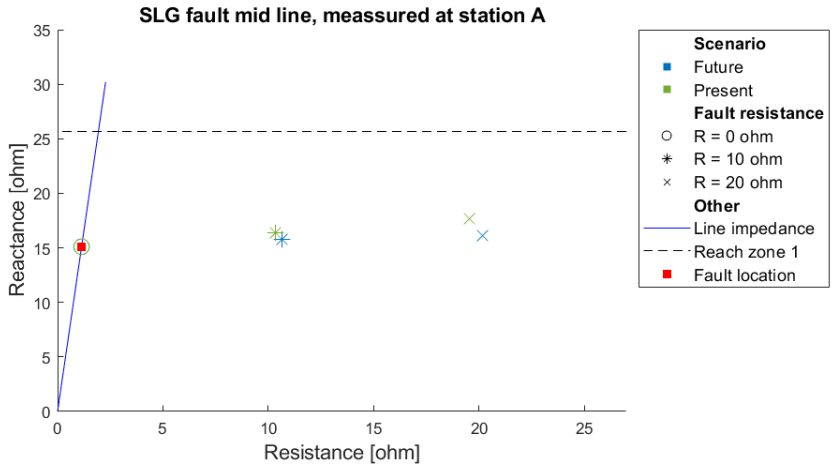

(a) Measured at station A.

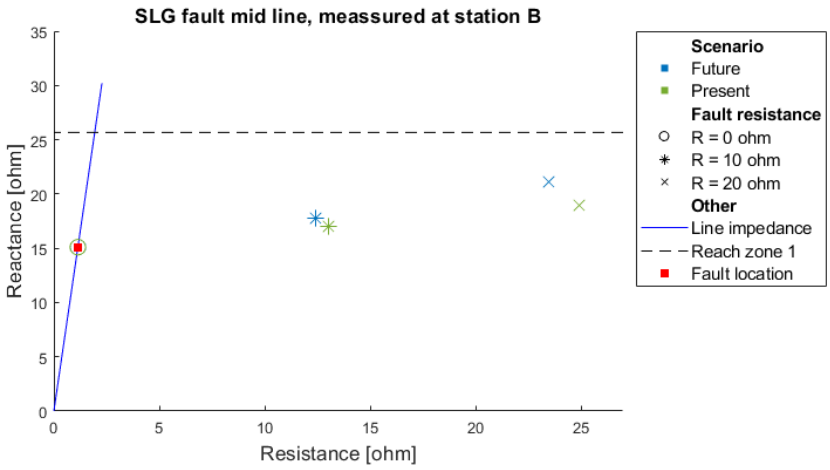

(b) Measured at station B.

Figure 8.7: SLG fault midline AB, with different impedances.

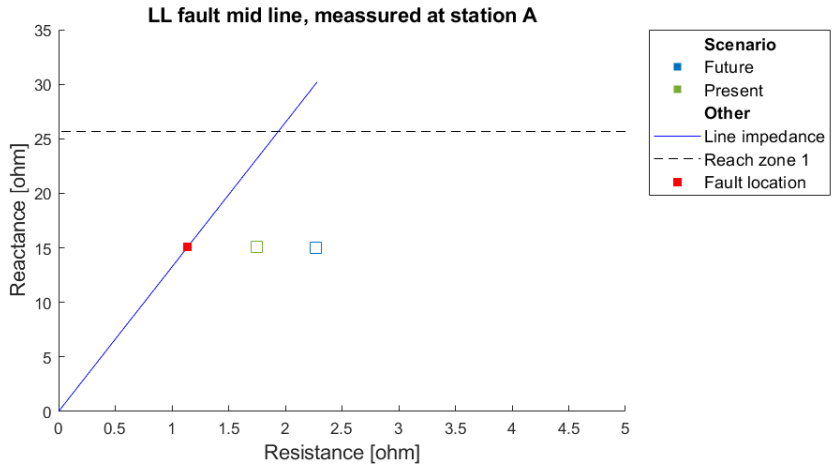

(a) Measured at station A.

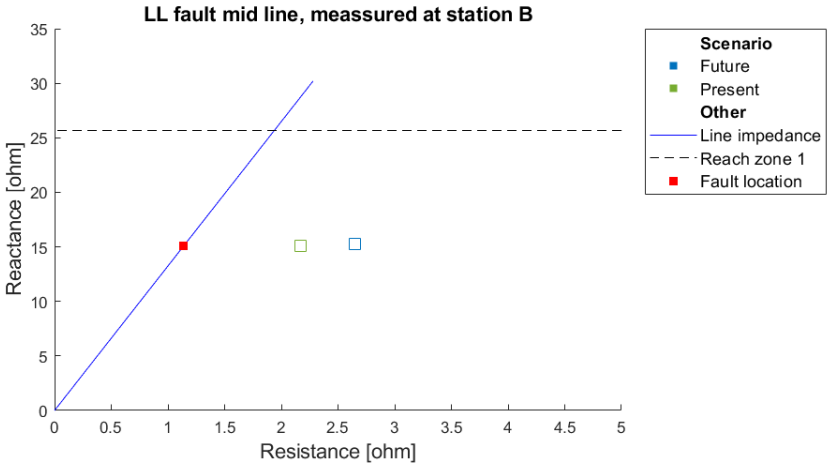

(b) Measured at station B.

Figure 8.8: LL fault midline AB, with arc resistance presented in table 8.3.

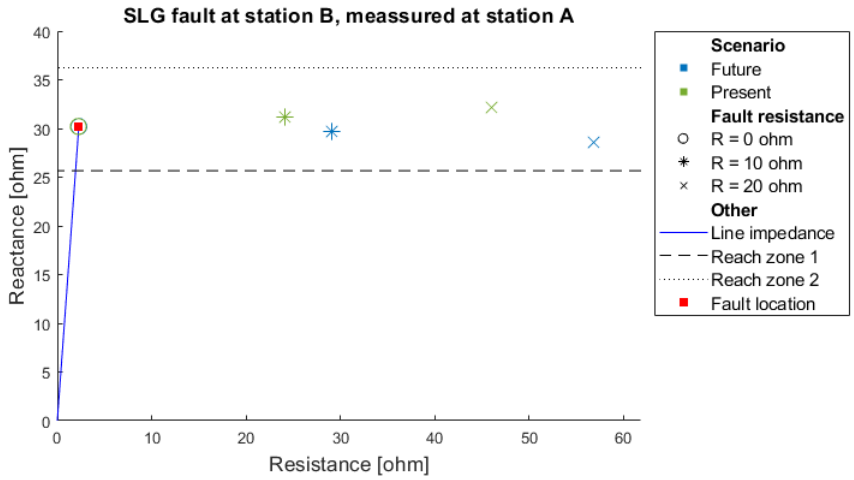

Figure 8.9: SLG faults at station B, with different fault resistance, measured at station A.

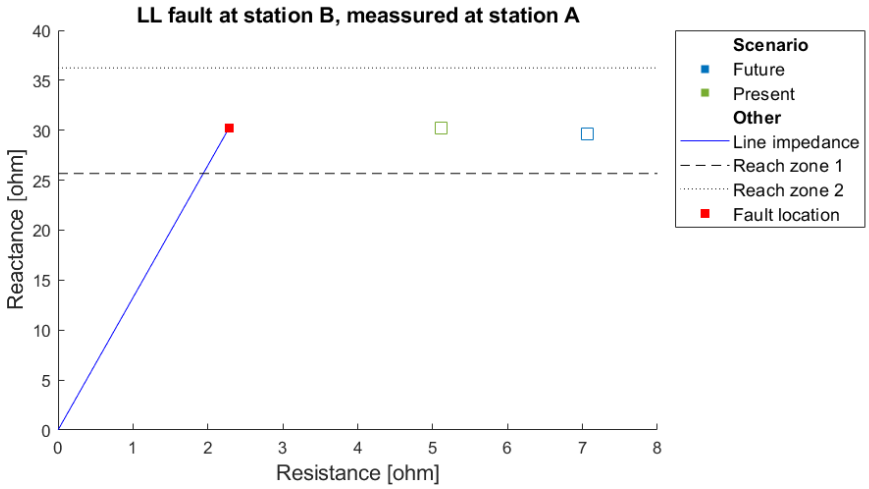

Figure 8.10: LL fault at station B with arc resistance presented in table 8.3, measured at station A.

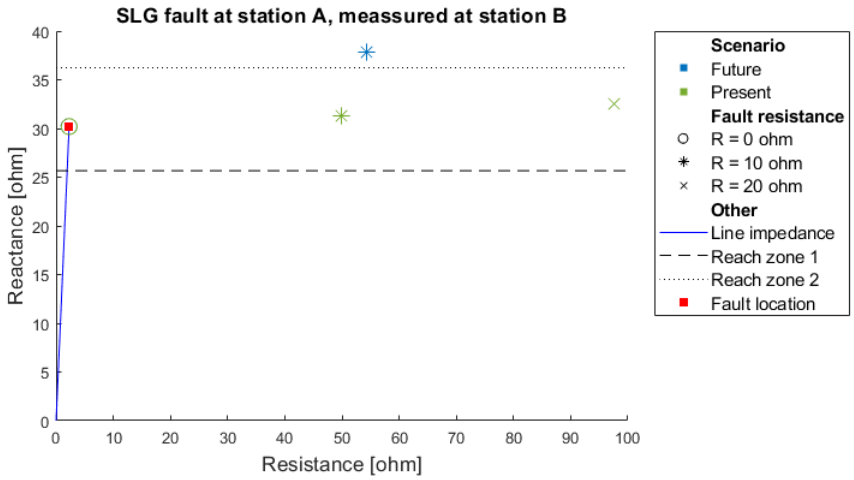

Figure 8.11: SLG fault at station A, measured at station B. SLG20 future is missing due to modelling issues.

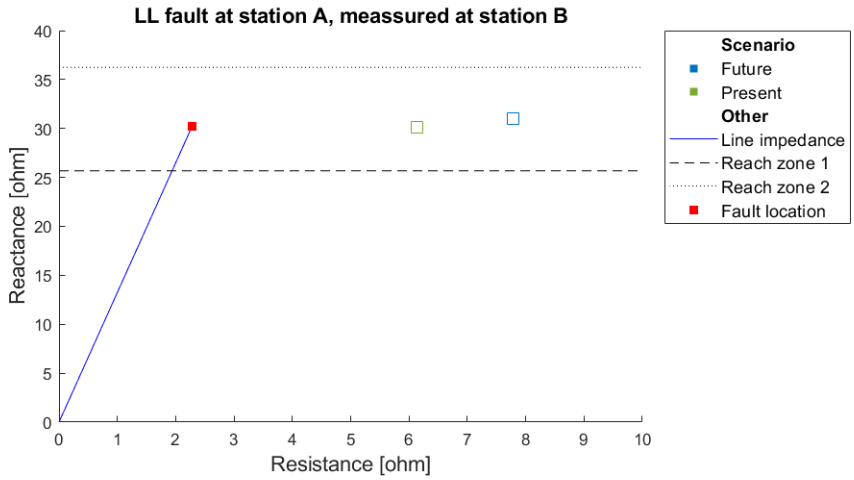

Figure 8.12: LL fault at station A with arc resistance presented in table 8.3, measured at station B.

Table 8.3: Arc resistance used in LL fault simulations.

Fault location	Future [Ohm]	Present [Ohm]
Midline	1.30	0.76
Station A	2.17	1.23
Station B	3.28	2.39

The result show that the apparent impedance does not differ significantly between the present and future scenario. This is likely because the capacity of synchronous generators is still significant due to hydro and thermoelectric power, even if nuclear power is shut down in the future. This indicates that general and overall actions may not be necessary for impedance settings of distance protection in high PEID penetrated

systems. However, as the result is based on current and voltage two cycles after the fault, no conclusion can be made regarding if fast protection functions (zone 1 for example) will work properly or not, if non steady-state properties is used to make tripping decisions.

8.3.2 Secundary voltage levels with varying line length

This section investigates how the system strength differs between the present power system model and the possible future model. In this case, the investigated line (line AB) is a part of a large meshed grid. Figure 8.13 and 8.14 displays secundary voltage at station A and B respectively, as a function of line length, for different fault types at station at the opposite station of line AB. As previously mentioned, the secundary voltage shall not fall below 5 V in order to ensure measuring accuracy [47].

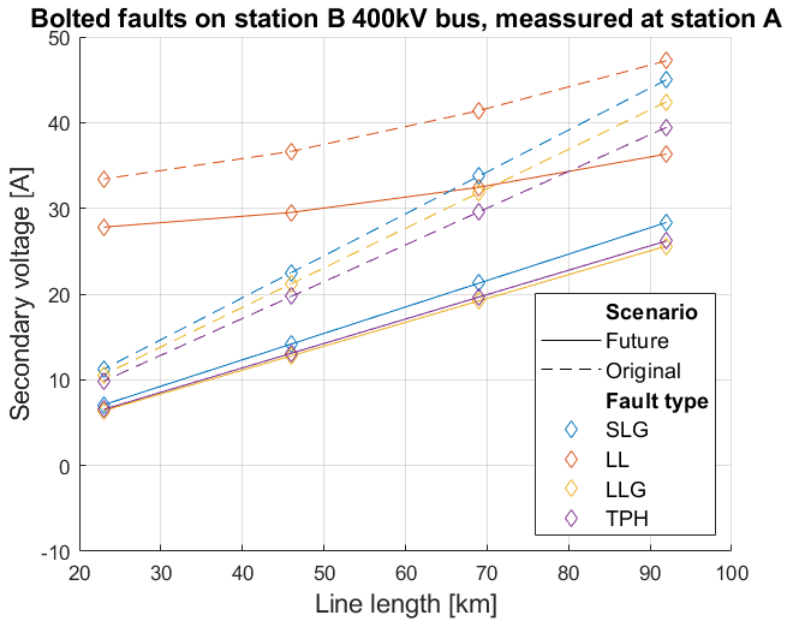

Figure 8.13: Voltage at station A as a function of line length, for different fault types at station B.

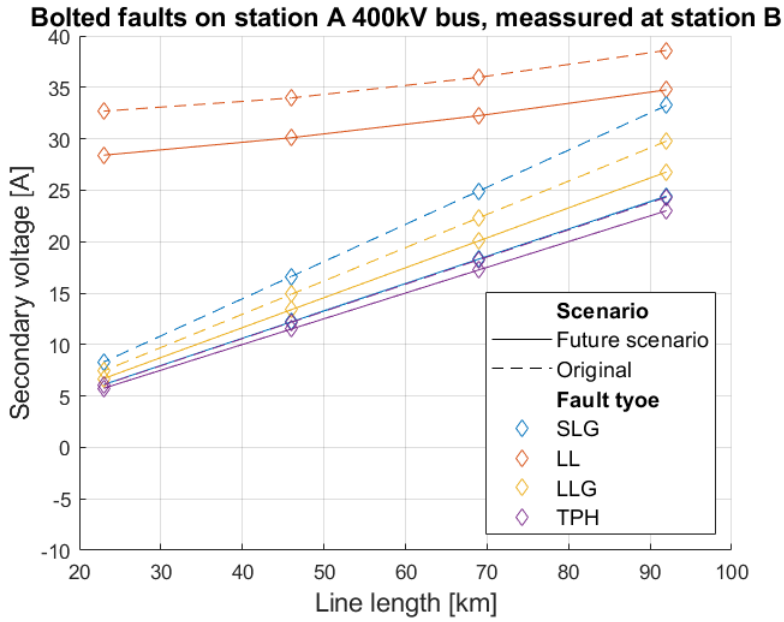

Figure 8.14: Voltage at station B as a function of line length, for different fault types at station A.

The result shows that the voltage does not risk falling below 5V for long nor short transmission lines in the investigated future scenario, at this specific location. This indicates that Svk:s rule of thumb regarding using line differential protection only for lines shorter than 25 km works in this future scenario, if only the voltage is taken into account.

As previously described, this future scenario is based on the assumption that large-scale RES increases dramatically and all nuclear power plants are shut down. If distributed RES on low voltage levels characterizes power production in the future at the same time as nuclear power plants are shut down, it can be assumed that this result does not hold, but further investigations of such systems is out of scope of this thesis.

8.3.3 Impact of intermediate infeed on the computed impedance

The following section will present results from investigations on the impact of intermediate infeed from PEID:s on zone 2 and zone 3 impedance calculations. The impedance is measured at station B, and faults are applied on two locations on the line between station A and C, displayed in figure 7.3. More specifically, fault are applied 60% and 99% from station A. The 60% mark is chosen in order to check that zone 2 of the distance protection at station B does not cover faults covered by zone 2 at station A. Moreover, the 99% mark is chosen in order to check whether or not zone 3 at station B covers the full line AC, which is should. Figure 8.15 shows the difference between infeed from traditional sources in the original scenario and from mainly PEID:s in the future scenario and figure 8.16 shows the same for LL faults. Table 8.4 presents arc resistance used for non-zero LL fault simulations.

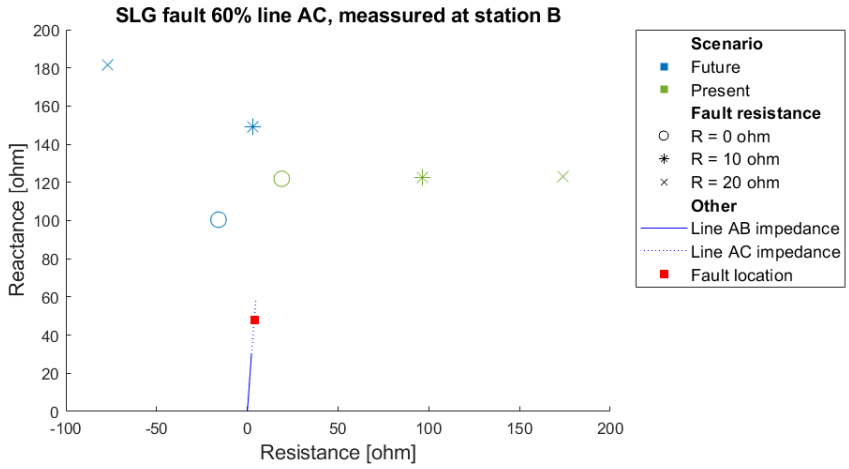

(a) Fault located 60% from station A.

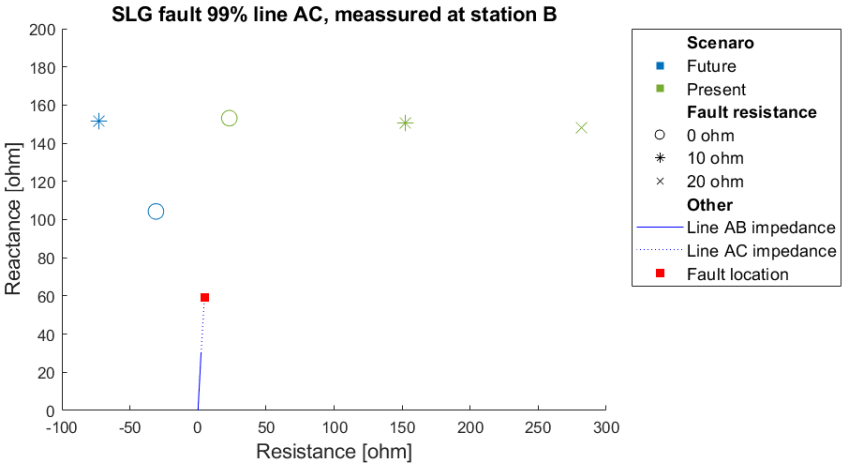

(b) Fault located 99% from station A.

Figure 8.15: Impedance measured at station B, for SLG faults on line AC.

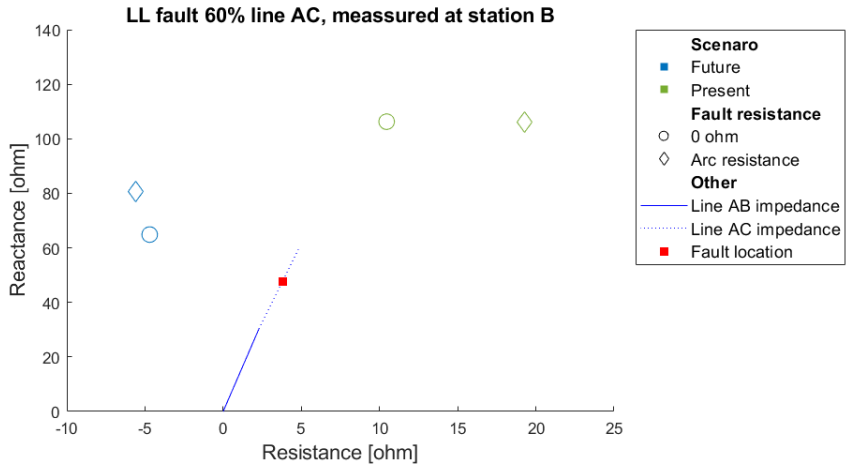

(a) Fault located 60% from station A.

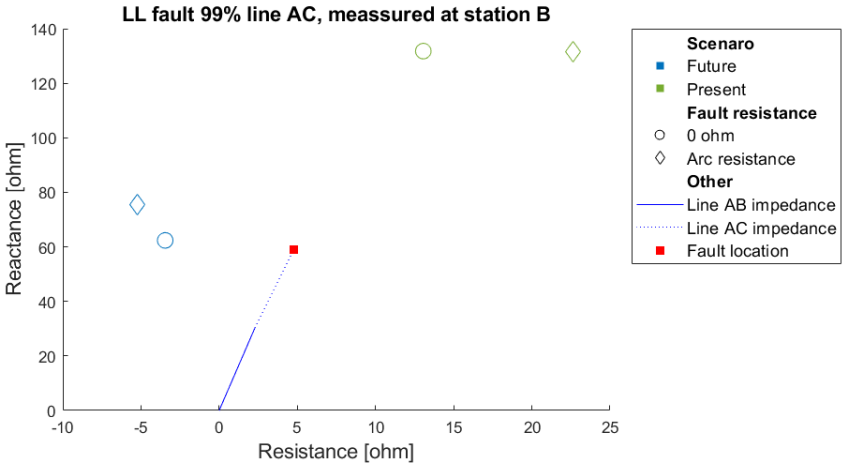

(b) Fault located 99% from station A.

Figure 8.16: Impedance measured at station B, for LL faults on line AC, with arc resistance presented in 8.4.

Table 8.4: Arc resistance used in LL fault simulations.

Fault location	Future [ohm]	Present [ohm]
60% line AC	3.35	1.84
99% line AC	2.36	1.36

It is clear trough comparing the future and original scenario, independently of fault location and resistance, that the impact from PEID infeed is very different compared to infeed from traditional sources. The most prominent difference being that PEID:s are capable of shifting the computed impedance to the negative R-axis. This is a phenomenon not occurring in traditional power systems.

From equation 8.2, it can be seen that the added impedance is dictated by the ratio of the intermediate infeed

and the local current measurement. If these quantities are equal in phase angle, the angle of the additional impedance is determined by the line impedance from the remote station to the fault point. In this case, the impedance up to the fault point on line AC, which is $Z_{AF} = (29.3 \angle{+}85°) \cdot X$, where X is the distance to the fault in percentage from station A. If there instead is a large phase angle difference between the the infeed and local current, the angle of the additional impedance is determined by both the current ratio and the line impedance. In this case, if the phase angle difference between the infeed and local current is greater than 5 °and smaller than 270 °, the calculated impedance will fall within the second or third quadrant in the impedance plane, where the additional impedance will consist of a negative part. The phase angle difference lays within this range in most fault scenarios presented in above figures.

Table 8.5 presents variables from the LL R=0 ohm case, at 60% from station A, which is used in an example calculation below. For a LL fault between phase a and b, the additional impedance can be calculated using equation 8.2, where $I_{b,local}$, $I_{c,local}$, $I_{b,infeed}$ and $I_{c,infeed}$ are the local and intermediate infeed current in phase a and b. Z_{AF} is as previously mentioned the line impedance from station B to the fault point.

Table 8.5: Current and line data for a LL fault on line BC, located 60% from station A.

Parameter	
Z_{AB} [ohm]	30.2859 $\angle$85.6825 °
Z_{AF} [ohm]	17.603 $\angle$85.05 °
$I_{b,local}$ (at station B) [A]	1425.0 $\angle{-}$158.9 °
$I_{c,local}$ (at station B) [A]	1583.4 $\angle$40.10 °
$I_{b,infeed}$[A]	2204.9 $\angle{-}$109.9 °
$I_{c,infeed}$[A]	1080.9 $\angle$46.75 °

$$Z_{app} = Z_{AB} + Z_{AF} + \underbrace{\frac{I_{b,infeed} - I_{c,infeed}}{I_{b,local} - I_{c,local}} \cdot Z_{AF}}_{\text{additional impedance}} \tag{8.2}$$

Inserting the variables above in the equation gives:

$$Z_{app} = 30.2859\angle 85.6825° + 17.603\angle 85.05° + \frac{1425.0\angle -158.9° - 1583.4\angle 40.10°}{2204.9\angle -109.9° - 1080.9\angle 46.75°} \cdot 17.603\angle 85.05°$$

$$= 47.8882\angle 85.45° + \underbrace{1.0872\angle 31.37°}_{\text{current ratio}} \cdot 17.603\angle 85.05°$$

$$= 47.8882\angle 85.45° + 19.137\angle 116.4°$$

$$= 65.0493\angle 94.1523°$$

$$= -4.7194 + j64.8746 \text{ [ohm]}$$

Negative impedance does not occur in traditional networks because the fault current phase angle is generally between 80-90 °as preciously mentioned, which means that the infeed and local current are close in phase. As described in section 4.3.1 and as seen in this section, this does not hold for PEID:s as the fault response is dictated by the controller. Therefore, this new type of intermediate infeed has to be taken into account for zone 2 and zone 3 distance protection settings in some grid topologies, for example in highly PEID penetrated systems.

Chapter 9

Discussion

This chapter aims to tie the result together and provide a further discussion on the implications of the result. First, the simulation methodology is discussed. Next, protection recommendations for radial lines connecting PEID:s are presented, followed by recommendations for highly PEID penetrated meshed networks. Lastly, a short discussion on the relevance of island operation with HVDC is included.

Simulation methodology

In this thesis project, simulations were conducted in the steady-state short circuit program PSS®CAPE. While this choice limited the amount of possible investigations as opposed to doing simulations in the time domain, this was the preferred option given the combined advantage of being able to use Svk:s main short circuit model, therefore decreasing needed modelling time, as well as being able to explore PSS®CAPE:s new type IV WTG model. In addition, the literature review is a significant part of this thesis and has provided answers to questions related to the protection performance prior to steady state.

Sub-grid 1 and sub-grid 2 was modelled in order to conduct investigations on radially connected PEID:s and on a highly PEID penetrated meshed network. As previously mentioned, sub-grid 2 is loosely based on the scenario *Renewable electrification* from Svk:s newest long-term market analysis, but due to assumptions and simplifications made, this model should be treated as just an example of a high PEID penetrated meshed network. Furthermore, a mix between type III and type IV is likely to be integrated to the power system in the future, but sub-grid 2 only consist of type IV WTG models. PSS®CAPE has a type III model, but because it is modelled as a current limited SG and therefore does not take into account voltage or crowbar dependency, it was not used. In addition, other not yet invented/not yet commercially available PEID:s, such as grid-forming converters for example, could also be integrated to the power system in the future. This decreases the "realness" of this future model. One limitation with the type IV WTG model is that negative sequence current injection is not available, removing the possibility to investigate how this affects steady-state current, voltage and apparent impedance.

As previously mentioned, the used type IV WTG model were thoroughly validated against EMTP simu-

lations by the model developer in reference [17]. As only small changes was made to Svk:s short circuit model in sub-grid 1a (only adding the type IV model and removing the LV-MV transformer), no further model validation was considered necessary. This was not performed in the case of sub-grid 2 either, as all lines, buses, auto-transformers and type IV WTG:s were copied from sub-grid 1a. However, simulation and computational result was spot-checked.

Protection of radial lines integrating PEID:s to the grid

This section will summarise identified protection challenges from the literature review and the simulation result in the case of radially integrated PEID:s. It will also discuss mitigation strategies. The discussion applies specifically to scenarios where PEID:s are integrated radially in a N-1 scenario. If PEID:s are integrated radially in normal operation, direct transfer trip from the strong line end can be used to obtain fast fault clearing along the whole line, without risking the selectivity. Figure 9.1 is used to explain some concepts in this section.

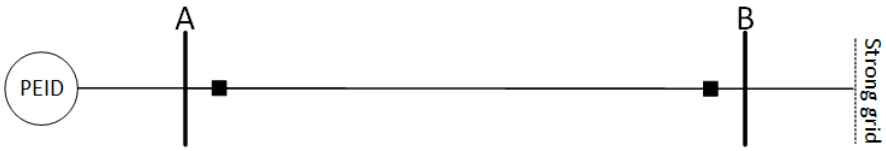

Figure 9.1: An example of a transmission line that integrates a PEID to a strong grid radially.

Some directionality and fault identification algorithms may limit the use of distance protection at bus A. This can be caused by the use of phasors from the transition period or the lack of negative sequence current injected by PEID:s in steady-state. The use of memory-polarized voltage will also increase the risk of misoperation of distance protection if the PEID is allowed to produce phase angle jumps. It is clear that a detailed understanding of included sub-functions in distance protection is needed, in order to choose the most suitable protection scheme for radial lines connecting PEID:s to the transmission grid. Information on the PEID control strategy would further improve protection planning of such topologies.

If the directionality algorithm, fault identification logic and voltage polarization are reliable, distance protection can be used on the line emanating from bus A. As shown in figure 8.2, high impedance faults can cause zone 1 to overreach 40 ms after the fault, as PSS®CAPE models the steady-state response two cycles after fault inception. Moreover, the voltage can reach low levels where the measuring accuracy of voltage is jeopardized as discussed in section 8.1.2. Therefore, the possibility of disabling zone 1 at bus A should be explored in some installations, for example where PEID:s are integrated using short transmission lines. In order to obtain fast fault clearance of zone 1 faults, a POTT scheme with weak infeed logic and transfer trip from the distance protection at bus B can be used. However, if the voltage risk falling below the minimum voltage needed to ensure the accuracy of measurement equipment, like for shorter line in figure 8.5a and 8.5b, line differential protection is a better option. The remaining protection strategy used by Svk does not have to change, e.g. the use of residual overcurrent protection on both sides of the line and distance protection at the line end interfacing bus B.

If the directionality algorithm, fault identification logic and voltage polarization are not reliable, the use of distance protection on the line end emanating from bus A is not recommended. Instead, line differential protection can be used as primary protection for short and long transmission lines. This does not cover faults between the current transformer and bus B, and therefore, direct transfer trip should be used from either the breaker failure and/or the busbar protection at bus B. Moreover, residual overcurrent protection can be used on both sides of the line and distance protection can be used like normal at the line end interfacing bus B. The protection scheme just explained is very communication dependent and the use of separate communication channels for the primary and local back-up protection is essential.

Protection in meshed power systems with a high penetration of PEID:s

Sub-grid 2 was modelled in order to make investigations in a high PEID penetrated network. The result showed small differences compared to the model representing the current transmission system in the case of measured voltage and impedance calculation without intermediate infeed, likely because thermal and hydro power contributes with short circuit power in addition to the added RES in this model. The transition period of the PEID response and the lack of negative sequence current injection by them may have less impact as well, which indicates that distance protection can be used in highly PEID penetrated meshed networks if a significant capacity of SG:s is also present. However, the investigation on intermediate infeed revealed nontraditional impedance calculations, e.g. negative resistance. Therefore, the possibility of expanding the zone 2 and 3 quadrilateral characteristic to the negative X-axis, which represents resistances, should be explored. On the other hand, due to the increased complexity of settings for zone 2 and 3 in presence of significant intimidate infeed from PEID:s, the need for remote back-up could be reevaluated. As Svk normally has local back-up protection, the need for remote back-up is not that significant. Furthermore, it should be noted that investigations were only conducted on one specific line and more investigations on other transmission lines and in other scenarios are needed. Investigations of very low short circuit power scenarios are especially interesting.

Protection during island operation with HVDC

Island operation of HVDC has not been in focus for this work. However, this is still related to the topics investigated in this thesis as it can be seen as the most extreme case of a PEID penetrated network. Some of the results from this work can probably be applied for islanded networks since the grid operated in this mode is still equipped with standard protections. These protections must be able to perform correctly with fault current from one converter only. Moreover it is reasonable to expect resemblance in challenges for protection functions identified in this work with challenges for protections during HVDC island operation. A summary of Svk:s experience from testings of this type of network are therefore included in appendix B. This will hopefully inspire further studies on the topic and also contribute with some practical experience.

Chapter 10

Future work

This thesis has, in general terms, summarized findings in the literature and performed steady-state simulations in order to improve the understanding of how PEID:s impact transmission line protection. It was found that some distance protection may misoperate in presence of PEID:s, but as previously mentioned, distance protection from different vendors and sometimes even different year of manufacturing from the same vendor, work differently. Therefore, the next step should be to evaluate the performance of specific distance protection more in detail, especially protection already installed close to PEID:s in the transmission system. This could for example be done using RTDS tools. In this way, the impact of the full PEID transient response can be investigated. For example with and without negative sequence current injection. The outcomes from these investigations can thereafter be used to define requirements for new protection installations.

Among reviewed literature in this thesis, only reference [5] presented observations from real disturbances, and the rest investigated the impact of PEID:s on protection using either RTDS or EMTP simulations. Although these simulations accurately represents the theoretical response of PEID:s, protection performance under real faults would further strengthen the understanding, as practice sometimes differ from theory. One example where this was the case was Svk:s black start capability test of a HVDC converter presented in appendix B. It is therefore recommended to save and analyse fault records from disturbances occurring on transmission lines emanating from PEID installations. If information on PEID pre-fault state and converter control strategy is available too, it is likely that valuable lessons can be learned. This could for instance be achieved in collaborations with distribution system operators or wind farm owners.

As previously mentioned, there is no grid code in Sweden specifying requirements for fault current injection by PEID:s. The development of such grid codes will likely be driven by needs of voltage support or other system stability related areas, but it is important that new requirements are evaluated from a protection perspective too. Therefore, future work is needed to learn what fault current characteristics will improve protection performance and/or what control strategy related information is needed to facilitate easier protection planning for equipment in presence of PEID:s.

The scope of this thesis was limited to overhead line protection. For future work, it could be interesting to investigate if there are more to learn about cable, transformer and busbar protection in presence of

PEID:s. Furthermore, this thesis has not included protection of series compensated lines. Protection of these transmission lines are more difficult in general, but the interaction between series compensation and PEID:s may cause even greater challenges. Basic characteristics of the interaction between these, caused by subsynchronous resonance, are described in [48] for example. Therefore, research related to protection of compensated transmission lines integrating PEID:s radially is suggested for future work.

The highly PEID penetrated meshed network studied in this thesis was not a particularly low inertia system and the conclusions made is likely not applicable in those cases. Thus, investigations of protection performance in very low inertia systems is an important area for future work. Protection solutions for islanded parts of the power system is another topology not included, e.g. when one or more PEID:s becomes isolated from the rest of the power system and continues to serve loads separately from the rest of the grid. This can occur intentionally and unintentionally as a result of outages in the power system, and protection of both types of islanded networks are areas in need of more investigations.

Chapter 11

Conclusions

Some general PEID fault response characteristics that are relevant from a protection perspective are low fault current magnitude, lack of or reduced negative sequence current for unbalanced faults, a wide range of possible current phase angles and the possibility of voltage phase angle jumps occurring. Information on the PEID strategy would facilitate well-founded protection schemes for transmission lines emanating from PEID:s. This information could be gained for example in collaboration with relevant generation plant owners or trough the establishment of grid codes that specifies requirements for fault current injection. Furthermore, it is important to take the response envolvement into account as many protection functions operate before steady-state is reached. The most critical part is the transition period, as oscillations in magnitude and phase angle of the injected current can occur during this stage, making phasor estimations less reliable.

Line differential protection and residual overcurrent protection works well in presence of PEID:s, but it is not apparent if all distance protection will when PEID:s are the only fault current source behind the protection. Radially connected PEID:s cannot be equated with a weak SG source in all operation modes. It is clear that Svk needs to learn more about distance protection used in the Swedish transmission system in order to ensure their functionality in presence of PEID:s. This includes improving their understanding of directional and fault identification algorithms, either by doing their own RTDS tests or trough collaboration with vendors. Furthermore, if distance protection are not reliable, the protection scheme of transmission line integrating PEID:s radially will likely be dependent on communication in order to cover all faults on the line. Furthermore, one prominent protection type which is not used by Svk currently is traveling wave protection. It is suitable in low inertia systems and in presence of PEID:s due to its high speed and non-fault current dependency. However, this type of protection may also be dependent on communication.

Bibliography

[1] WindEurope. 2020 Statistics and the outlook for 2021-2025. 2021. URL: https://windeurope.org/intelligence-platform/product/wind-energy-in-europe-in-2020-trends-and-statistics/ (visited on 05/27/2021).

[2] Mattias Johnsson et al. Långsiktig marknadsanalys 2021. 2021. URL: https://www.svk.se/siteassets/om-oss/rapporter/2021/langsiktig-marknadsanalys-2021.pdf.

[3] Christian Holmström. Elproduktion. 2021. URL: https://www.ekonomifakta.se/fakta/energi/energibalans-i-sverige/elproduktion/ (visited on 05/22/2021).

[4] Sandra Thengius. "Fault current injection from power electronic interfaced devices". MA thesis. KTH Royal institute of technology, Sept. 2020.

[5] Mukesh Nagpal et al. "Protection Challenges and Practices for Interconnecting Inverter Based Resources to Utility Transmission Systems". In: IEEE Power Energy Society (July 2020), p. 64.

[6] Moumita Sarkar, Jundi Jia, and Guangya Yang. "Distance relay performance in future converter dominated power systems". In: 2017 IEEE Manchester PowerTech. 2017, pp. 1–6. DOI: 10.1109/PTC.2017.7981144.

[7] Ankita Roy and Brian K. Johnson. "Transmission side protection performance with Type-IV wind turbine system integration". In: 2014 North American Power Symposium (NAPS). 2014, pp. 1–6. DOI: 10.1109/NAPS.2014.6965429.

[8] Shawn M Holder, Li Hang, and Brian K Johnson. "Investigation of transmission line protection performance in an electric grid with electronically coupled generation". In: 2013 North American Power Symposium (NAPS). IEEE. 2013, pp. 1–6.

[9] EEEGUIDE. Fault Resistance Calculation. n.d. URL: https://www.eeeguide.com/fault-resistance-calculation/ (visited on 05/16/2021).

[10] J Duncan Glover, Mulukutla S Sarma, and Thomas Overbye. Power system analysis & design, SI version. 5th ed. Cengage Learning, 2012.

[11] Michael Bergstrom et al. Network Protection and Automation Guide - Protective Relays, Measurement and Control. 6th ed. Alstom Grid, May 2011. ISBN: 978-0-9568678-0-3.

[12] Svenska Kraftnät. TR02-05-2-2: Distansskydd. Dec. 2013. URL: https://www.svk.se/siteassets/4.aktorsportalen/natverksamhet/tekniska-riktlinjer/tr02/1tr02-05-2-2-5-2013-12-10.pdf.

[13] The International Renewable Energy Agency. Renewable Electricity Capacity and Generation Statistics, March 2021. 2021. URL: https://www.irena.org/Statistics/View-Data-by-Topic/Capacity-and-Generation/Statistics-Time-Series (visited on 05/24/2021).

[14] "Fault current contributions from wind plants". In: 2015 68th Annual Conference for Protective Relay Engineers. 2015, pp. 137–227. DOI: 10.1109/CPRE.2015.7102165.

[15] Hussain Alharthi et al. "Evaluation of Distance Protection Responses in AC Power System With Converter Interface". In: 2019 IEEE Innovative Smart Grid Technologies - Asia (ISGT Asia). 2019, pp. 2270–2275. DOI: 10.1109/ISGT-Asia.2019.8881574.

[16] Zhou Xiaojie and Ruan Yi. "Modeling and simulation analysis of 3-level VSC-STATCOM based on SVPWM". In: 2011 IEEE Power Engineering and Automation Conference. Vol. 2. 2011, pp. 111–114. DOI: 10.1109/PEAM.2011.6134920.

[17] Athula Rajapakse et al. "Modification of Commercial Fault Calculation Programs for Wind Turbine Generators". In: IEEE Power Energy Society (June 2020), p. 81.

[18] Evangelos Farantatos et al. Impact of Inverter-Based Resources on Protection Schemes Based on Negative Sequence Components. EPRI and Polytechnique Montreal, July 2019.

[19] Aboutaleb Haddadi et al. "Impact of Inverter Based Resources on System Protection". In: Energies 14 (Feb. 2021), p. 1050. DOI: 10.3390/en14041050.

[20] D López et al. "Negative sequence current injection by power electronics based generators and its impact on faulted phase selection algorithms of distance protection". In: (2018).

[21] E. Martínez et al. "Effects of Type-4 Wind Turbine on present protection relaying algorithms". In: Migrate project (2018).

[22] Gustav Steynberg. Challenges and solutions for distance protection in systems with high penetration of converter-based generation. Siemens World of Energy Automation – Protection User Conference. May 2021.

[23] Aboutaleb Haddadi et al. "Impact of Inverter-Based Resources on Memory-Polarized Distance and Directional Protective Relay Elements". In: 2020 52nd North American Power Symposium (NAPS). 2021, pp. 1–6. DOI: 10.1109/NAPS50074.2021.9449791.

[24] Yingyu Liang, Wulin Li, and Guanjun Xu. "Performance Problem of Current Differential Protection of Lines Emanating from Photovoltaic Power Plants". In: Sustainability 12.4 (Feb. 2020), p. 1436. ISSN: 2071-1050. DOI: 10.3390/su12041436. URL: http://dx.doi.org/10.3390/su12041436.

[25] Subhadeep Paladhi and Ashok Kumar Pradhan. "Adaptive Distance Protection for Lines Connecting Converter-Interfaced Renewable Plants". In: IEEE Journal of Emerging and Selected Topics in Power Electronics (2020), pp. 1–1. DOI: 10.1109/JESTPE.2020.3000276.

[26] Amin Banaiemoqadamfariman. "Distance Protection Challenges of Converter-Interfaced Renewable Energy Sources". MA thesis. Toronto, Ontario: York University, Aug. 2018.

[27] Power system protection solutions for future transmission networks. Tech. rep. The migrate project, Nov. 2020. URL: https://www.h2020-migrate.eu/downloads.html.

[28] Alexander Novikov, Jose Jesus de Chavez, and Marjan Popov. "Performance Assessment of Distance Protection in Systems with High Penetration of PVs". In: 2019 IEEE Milan PowerTech. 2019, pp. 1–6. DOI: 10.1109/PTC.2019.8810491.

[29] Juergen Holbach et al. "Protection functionality and performance with declining system fault levels and inertia within national grid electricity transmission system in the United Kingdom". In: 15th International Conference on Developments in Power System Protection (DPSP 2020). 2020, pp. 1–6. DOI: 10.1049/cp.2020.0065.

[30] Felipe Wilches-Bernal et al. "A Survey of Traveling Wave Protection Schemes in Electric Power Systems". In: IEEE Access 9 (2021), pp. 72949–72969. DOI: 10.1109/ACCESS.2021.3080234.

[31] Sinisa Zubic, Zoran Gajic, and Davor Kralj. "Line Protection Operate Time: How Fast Shall It Be?" In: IEEE Access 9 (2021), pp. 75608–75616. DOI: 10.1109/ACCESS.2021.3081993.

[32] Protection Challenges for the Changing Electrical Grid. Tech. rep. Siemens AG, 2019.

[33] ENTSO-E. Use of travelling waves principle in protection systems and related automations. Tech. rep. May 2021.

[34] Edmund O Schweitzer et al. "Speed of line protection-can we break free of phasor limitations?" In: 2015 68th Annual Conference for Protective Relay Engineers. IEEE. 2015, pp. 448–461.

[35] Mohd Asim Aftab et al. "Dynamic protection of power systems with high penetration of renewables: A review of the traveling wave based fault location techniques". In: International Journal of Electrical Power & Energy Systems 114 (2020), p. 105410.

[36] Bogdan Kasztenny et al. "Practical setting considerations for protective relays that use incremental quantities and traveling waves". In: 43rd Annual Western Protective Relay Conference, Washington, USA. 2016.

[37] Eduardo Martınez Carrasco et al. "Improved faulted phase selection algorithm for distance protection under high penetration of renewable energies". In: Energies 13.3 (2020), p. 558.

[38] M. Singh and V. Telukunta. "Adaptive distance relaying scheme to tackle the under reach problem due renewable energy". In: 2014 Eighteenth National Power Systems Conference (NPSC). 2014, pp. 1–6. DOI: 10.1109/NPSC.2014.7103785.

[39] ENTSO-E. Adaptive Protection Technology. n.d. URL: https://www.entsoe.eu/Technopedia/techsheets/adaptive-protection-technology (visited on 07/07/2021).

[40] Vishnuvardhan Telukunta et al. “Protection challenges under bulk penetration of renewable energy resources in power systems: A review”. In: CSEE journal of power and energy systems 3.4 (2017), pp. 365–379.

[41] Uma Uzubi, Arthur Ekwue, and Emenike Ejiogu. “Adaptive distance relaying: Solution to challenges of conventional protection schemes in the presence of remote infeeds”. In: International Transactions on Electrical Energy Systems 30.5 (2020), e12330.

[42] Rahul K Dubey, Subhransu Ranjan Samantaray, and Bijay Ketan Panigrahi. “Adaptive distance relaying scheme for transmission network connecting wind farms”. In: Electric Power Components and Systems 42.11 (2014), pp. 1181–1193.

[43] A. K. Pradhan and Gza Joos. “Adaptive Distance Relay Setting for Lines Connecting Wind Farms”. In: IEEE Transactions on Energy Conversion 22.1 (2007), pp. 206–213. DOI: 10.1109/TEC.2006.889621.

[44] Khalil El-Arroudi and Géza Joós. “Performance of Interconnection Protection Based on Distance Relaying for Wind Power Distributed Generation”. In: IEEE Transactions on Power Delivery 33.2 (2018), pp. 620–629. DOI: 10.1109/TPWRD.2017.2693292.

[45] Roy Moxley and Farel Becker. “Adaptive protection—what does it mean and what can it do?” In: 2018 71st Annual Conference for Protective Relay Engineers (CPRE). 2018, pp. 1–4. DOI: 10.1109/CPRE.2018.8349769.

[46] Siemens Industry Inc. Inverter-Based Generator Models with Controlled Power and Current: 2020 CAPE User Guide. Oct. 2020.

[47] Tony Seegers et al. “AC Transmission Line Model Parameter Validation”. In: IEEE Power Energy Soc. (Sept. 2014), pp. 1–50.

[48] Einar V. Larsen. “Wind generators and series-compensated AC transmission lines”. In: PES T&D. 2012, pp. 1–4. DOI: 10.1109/TDC.2012.6281548.

Appendix A

Questionnaire sent to protection vendors

Background
An increasing deployment of power electronic-interfaced devices (PEID), like wind plants, solar plants, HVDC and FACTS, changes the power system fault response. Fault characteristics of PEID:s are significantly different compared to synchronous machines (SGs), for example the fault current is lower in amplitude, can be either capacitive, inductive and/or resistive and may be symmetric for asymmetric faults. These characteristics are heavily dependent on the grid side converter control. The purpose of the master thesis in question is to investigate how these changes affect the functionality of the existing protection system in the Swedish transmission grid and how potential problems can be mitigated.

Questions

Distance protection

- How does the distance protection directional algorithm work? Is it dependent on the negative sequence current/voltage? Do you predict that the risk of malfunction increases as the deployment of PEID increases?
- Do you have any recommendations regarding the distance protection zone 1 settings in a system where the deployment of PEID is high?
- Do you see any risk in distance protection being prone to misoperation with respect to fault type determination due to high PEID penetration? E.g. a single phase fault is seen by the relay as a phase to phase fault.
- How is the power swing blocking function in the distance protection affected by an increasing deployment of PEID?
- Do you recommend us to use any other type of distance protection function (compared to those we use today) in your IED in the future due to more PEID in the grid? If yes, which and why?

Differential protection

- Have you identified any problems in using line differential protection in a power system where the deployment of PEID is high? For example if capacitive fault current is injected by PEID.

General

- What protection schemes do you recommend for a 400 kV transmission line with
  a. One week end (PEID dominated) and one strong end (SG dominated)
  b. Two week ends (PEID dominated)
- Do you have any other insights about this topic to share?

Appendix B

Island operation with HVDC

Among Svk assets, there is one HVDC transmission connection with black start capability. It is called NordBalt and is connected to the Swedish transmission system via Nybro substation. A couple of years ago, Svk carried out verification tests of island operation at Nybro substation. Some of the tests were focused on verification of protection functions, but the test system was limited to the substation and with the now gained knowledge it is of interest to reevaluate the conclusions made after the test.

One conclusion made during the tests was that the fault current is very limited. For three-phase short circuit faults, the fault current was just above 600A. This is roughly 0.5 p.u. of the rated current of the converter. This is well above the current level of the 400 kV transmission line protection, as they operate down to 300A. However, it is lower than what has been noted in the literature reviewed in this thesis project. In addition, this thesis project has revealed additional conditions which has to be fulfilled in order to secure reliable protecting function, such as phase selection, direction determination, reach accuracy among other things. These are fully dependent on the control parameters of the converter. Based on these conclusions, additional protection verification tests, e.g. in RTDS environment, is strongly recommended.